QATAR UNIVERSITY

COLLEGE OF HEALTH SCIENCES

INVESTIGATION OF THE HUMORAL IMMUNE RESPONSES IN SARS-COV-2 INFECTED AND VACCINATED INDIVIDUALS

BY

HADEEL TAREQ MOHAMMED ZEDAN

A Thesis Submitted to

the College of Health Sciences

in Partial Fulfillment of the Requirements for the Degree of

Masters of Science in Biomedical Sciences

June 2022

COMMITTEE PAGE

The members of the Committee approve the Thesis of
Hadeel Tareq Mohammed Zedan defended on 24/04/2022.

Dr. Gheyath Khaled Nasrallah
Thesis/Dissertation Supervisor

Dr. Hadi Mohammed Yassine
Committee Member

Dr. Laith Abu Raddad
Committee Member

Dr. Atiyeh Abdallah
Committee Member

Dr. Patrick Tang
Committee Member

Approved:

Dr. Hanan F. Abdul Rahim, Dean, College of Health Science

ABSTRACT

ZEDAN, HADEEL, T., Masters of Science : April : 2022, Biomedical Sciences

Title: Investigation of the humoral immune responses in SARS-CoV-2 infected and vaccinated individuals.

Supervisor of Thesis: Dr. Gheyath K. Nasrallah

Background: Protective and lasting immunity to viral infections or vaccines are usually achieved through the combined actions of both cellular and humoral immune responses. Although there exists clear evidence supporting the importance of neutralizing antibodies (NAbs) in conferring protection in SARS-CoV-2 infected and vaccinated individuals, these NAbs responses wane rapidly over time and appear to be less effective against the new SARS-CoV-2 variants. In that case and given the myriad roles of antibodies, it can be presumed that antibodies could also mediate protection against SARS-CoV-2 via effector mechanisms such as antibody-dependent cellular cytotoxicity (ADCC), providing new correlates of protective immunity.

Objectives: This project aims to investigate and characterize the humoral immune responses in previously infected SARS-CoV-2 patients and COVID-19 vaccinated individuals to identify the correlates of protective immunity.

Methods: First, the performance of nine IgM and IgG ELISA kits, five automated immunoassays, and two surrogate virus neutralization tests (sVNT) was assessed using a wide range of sera samples collected from previously infected and vaccinated individuals. Then, humoral responses, including binding and NAbs, and ADCC activity against different SARS-CoV-2 antigens were characterized for a selected group of sera samples (n=90 from infected; n=77 from vaccinated individuals).

Results: We observed a heterogeneous assay performance for IgM serological assays, whereas IgG assays targeting the SARS-CoV-2 spike (S) protein showed a good to

excellent overall performance. Both sVNTs targeting the SARS-CoV-2 receptor binding domain (RBD) demonstrated excellent performance and correlation with the pseudovirus neutralization reference test. These results suggest that that these assays could serve as robust platforms for reliable and high-throughput screening of RBD-targeting NAbs. As for ADCC responses, it was shown that ADCC was elicited within the first 10 days post-infection and 30 days post-vaccination after the second dose and remained detectable after two months in both groups. Patients with severe disease had significantly higher ADCC levels against both the S and nucleocapsid (N) proteins than asymptomatic and vaccinated individuals. Notably, no significant difference in the ADCC levels was observed between individuals vaccinated with BNT162b2 and mRNA-1273 vaccines, despite binding antibody and NAbs responses being significantly higher in mRNA-1273-vaccinated individuals. Additionally, there was no significant difference in ADCC levels across the different age groups and between genders.

Conclusion: Several commercial immunoassays were identified as reliable assays for the detection of anti-SARS-CoV-2 humoral responses. The extent to which these conventional serology assays correlate with neutralization was shown to depend on the targeted antigen and on the time of sample collection post disease onset. Further, significant FcγR-binding ADCC response were detected in infected and vaccinated individuals but was more prominent in symptomatic COVID-19 patients, suggesting that ADCC assay could be used to estimate the extra-neutralization activity of antibodies targeting SARS-CoV-2.

ACKNOWLEDGMENTS

“I would like to express my special appreciation and gratitude to my supervisor, Dr. Gheyath Nasrallah, and my co-supervisor, Dr. Hadi Yassine, as well as my committee members for their guidance, insights, and continuous support throughout this research project. Also, I would like to express my sincere gratitude to my fellow lab members and friends, namely Ms. Maria Smatti, Dr. Hebah Al-Khatib, Ms. Duaa Al-Sadeq, and Ms. Fatma Ali. I would like to thank my friends and family as well for their unconditional support throughout my entire studying journey. In addition, I would like to acknowledge the support of Qatar University for providing all the needs to achieve the requirements of this study". I would like to also acknowledge funds from RRC-2-032 grant from the Qatar National Research Fund (a member of Qatar Foundation) and QUST-1-CHS-2021-15 grant from Qatar University. I would also like to thank Mindray Bio-Medical Electronics, China and bioMérieux Biotechnology, France, for their generous in-kind support with the reagents and the kits.

Table of Contents

LIST OF FIGURES

LIST OF TABLES

CHAPTER 1: INTRODUCTION

The severe acute respiratory syndrome coronavirus 2 (SARS-CoV-2) first emerged in Wuhan, China, in late 2019, causing an unprecedented outbreak of pneumonia, which was later termed coronavirus disease 2019 (COVID-19) by the World Health Organization (WHO) [1]. Despite the stringent containment and quarantine efforts during the beginning of the pandemic, the number of cases continued to increase, causing outbreaks in over 160 countries worldwide with a case-fatality rate of about 1-2% [2]. Compared to the severe acute respiratory syndrome coronavirus (SARS-CoV) and Middle East respiratory syndrome coronavirus (MERS-CoV), SARS-Cov-2 is more contagious and highly transmissible [3]. In addition, the rapid increase in SARS-CoV-2 cases overwhelmed healthcare systems and led to various public health measures to control the outbreak including restrictions in social and economic activities. Diagnostic testing played a large role in the management of the outbreak, including both tests that detect the virus as well as serology tests that measure immune responses to the virus and vaccine. The detection of the SARS-CoV-2 viral RNA by real-time reverse transcriptase-polymerase chain reaction (RT-PCR) remains the gold standard test for the diagnosis of COVID-19 [4]. However, it is expensive and demands sophisticated laboratory facilities and the sensitivity of the assay depends on the type and adequacy of sample, sampling technique, time of sample collection in relation to symptom onset, and viral load. Serological assays are important adjuncts for the diagnosis of COVID-19 in patients with persistent symptoms and can help identify convalescent individuals who have already developed an immunity against the virus, and therefore, may no longer be susceptible to infection [4-6]. Also, they provide additional value in seroprevalence studies to identify herd immunity and establish health control policies for controlling pandemics. However, most

commercially available serology assays cannot differentiate between the different types of antibodies (i.e., binding antibodies (non-protective) vs. functional/protective antibodies). Therefore, detection of anti-SARS-CoV-2 antibodies by these high throughput assays does not necessarily correlate with protection against infection, given that most of these binding antibodies are not protective [7, 8]. Further, most serological assays detect humoral responses, whereas assays that detect cellular responses are limited.

Following the declaration of SARS-CoV-2 as a pandemic by the WHO, several effective vaccines were rapidly developed and deployed globally [9]. These vaccines and other antiviral interventions were designed against the initial SARS-CoV-2 strain that emerged in 2019 [10]. Although some studies have shown that the developed vaccines can still induce an immune response against the new variants, these variants were not as sensitive to neutralization as the ancestral strain. Further, these studies also assessed how these mutations affect the immune system's recognition in previously infected and vaccinated individuals [11-13]. Such findings have created concerns regarding whether these variants could escape the vaccine-induced immunity and raised questions regarding the future evolutionary trajectories of SARS-CoV-2 variants. Therefore, there is a dire need for more studies to identify new correlations of protective immunity against SARS-CoV-2, which can be relied upon to identify individuals who are protected against infection or severe disease and inform the development of new antiviral drugs agents and vaccines.

Nevertheless, vaccinology research has always relied on the generation of neutralizing antibodies (NAbs) as the benchmark for developing and measuring the effectiveness of vaccines. However, neutralization alone is a modest predictor of protection [14-17]. Instead, there is increasing evidence suggesting a critical role for additional extra-

neutralizing functions of antibodies in protecting against infection. Specifically, beyond binding and neutralization, antibodies mediate various other immune functions via their ability to recruit and deploy innate immune effector functions [17-19]. This includes antibody-dependent cellular cytotoxicity (ADCC), which is an immune mechanism through which Fc receptor-bearing immune cells can recognize and kill antibody-coated target cells expressing tumor- or pathogen-derived antigens on their surface [14, 15, 17, 18, 20, 21]. Currently, there has been considerable interest in ADCC responses that activate cellular immune responses in addition to their neutralization activity. However, despite their big role in immunity, the characteristics and diagnostic value of ADCC responses produced in COVID-19 patients' sera and the antigens targeted by these antibodies have not been studied yet. Hence, evaluating the dynamics of SARS-CoV-2 specific protective antibody responses (NAbs and ADCC) to different SARS-COV-2 antigens is essential to identify the correlates of protection in previously infected and vaccinated individuals.

1.1 Objectives

The current project aims to assess the humoral immune responses against different SARS-CoV-2 antigens in previously infected and vaccinated individuals. Specific objectives include:

1. Evaluate the performance of different commercial immunoassays detecting antibodies against different SARS-CoV-2 antigens in infected and vaccinated individuals.
2. Perform full characterization of binding antibodies, NAbs, and ADCC responses among infected and vaccinated individuals.
3. Compare and correlate between the humoral immune responses targeting different SARS-CoV-2 antigens including the full spike (S) protein, receptor

binding domain (RBD), and nucleocapsid (N) protein.

4. Correlate ADCC activity with binding antibodies and NAbs with among infected and vaccinated individuals

CHAPTER 2: BACKGROUND

Coronaviruses, first discovered in the 1960s, are enveloped positive-sense single-stranded ribonucleic acid (RNA) viruses that belong to the order *Nidovirales*, family *Coronaviridae*, and the subfamily Coronavirinae (shown in Figure 1). These viruses have the largest genome among all RNA viruses and are characterized by their club-like crown shape formed by the spikes protruding from the surface [22]. The family *Coronaviridae* comprises over a dozen major host-specific pathogens that have the potential of infecting a wide range of mammals and birds, displaying tropism for the respiratory tract, the enteric tract, the liver, and the brain [23, 24]. Also, coronaviruses are an important cause of respiratory infections ranging from common cold to severe acute respiratory syndrome (SARS) [24]. The subfamily Coronavirinae is further classified into four main genera, Alpha-, Beta- Gamma-, and Deltacoronaviruses, based on the serological and genomic properties [25]. Human coronaviruses (HCoVs) either belong to the Alpha- or Betacoronavirus genera, including HCoV-229E and HCoV-NL63 (Alphacoronaviruses), and HCoV-HKU1, SARS-CoV, MERS-CoV, and HCoV-OC43 (Betacoronaviruses) as shown in Figure 1 [25].

2.1 Human coronaviruses

Among all discovered coronaviruses thus far, seven species are known to infect human hosts (also known as HCoV), causing mild to severe respiratory symptoms depending on the coronavirus's lineage and the immune status of the host [26]. The most recent coronavirus emergence incidence in the twenty-first century includes the severe acute respiratory syndrome coronavirus (SARS-CoV) [27] and Middle East respiratory syndrome coronavirus (MERS-CoV) [28], which caused significant morbidity and mortality in affected individuals, particularly the elderly patients [29, 30]. Until the outbreak of SARS-CoV in 2002 in China, coronaviruses were not

considered highly pathogenic to humans as they were only associated with mild infections in immunocompetent individuals [31]. Following the outbreak of SARS-CoV by ten years, another highly pathogenic coronavirus emerged in the Middle Eastern countries, which was later named MERS-CoV [32]. SARS-CoV infects ciliated bronchial epithelial cells and type II pneumocytes via angiotensin-converting enzyme 2 (ACE2) receptor [33], whereas MERS-CoV infects non-ciliated bronchial epithelial cells and type II pneumocytes via dipeptidyl peptidase 4 (DPP4) receptor [34].

Other common human coronaviruses include the four endemic subtypes: HCoV-229E, HCoV-NL63, HCoV-OC43, and HCoV-HKU1, which can cause mild to moderate upper-respiratory tract illness but use different receptor molecules with variable host cell tropism [35]. Although the epidemiology of SARS-CoV and MERS-CoV has been characterized by contained epidemics, seasonal HCoVs are endemic and widely spread worldwide, presumably contributing to 15%–30% of cases of common colds in humans [36, 37]. Unlike SARS-CoV, which spreads to the lower respiratory tract to cause a severe infection, HcoV-229E and HcoV-OC43 replicate primarily in the upper respiratory tract epithelial cells, causing local respiratory symptoms [37]. Further, individuals infected with seasonal coronavirus usually do not seek medical attention and there is a limited duration of viral shedding, making the detection of viral infection not useful for performing long-term epidemiological studies [38]. Moreover, the seroprevalence of the four seasonal coronaviruses tends to decline after waning of maternal antibodies after birth; however, it rises rapidly afterward and remains stable in adults due to the regular re-exposure to these viruses throughout life [39].

In MERS-CoV, antibody response was shown to be detectable 14-21 days after

infection and high concentrations increased over time remaining detectable for more than 18 months [40, 41]. Also, long-term antibody responses were sown to rely on the severity of MERS-CoV infection. As for SARS-CoV, antibody responses, they remain detectable up to two years after infection and then gradually decreased until completely disappearing 6 years after infection [42, 43]. Cellular immunity was also characterized and was shown to last longer than humoral responses , where SARS-specific memory T cells persisted in blood at 17 years post-infection in three recovered patients [44].

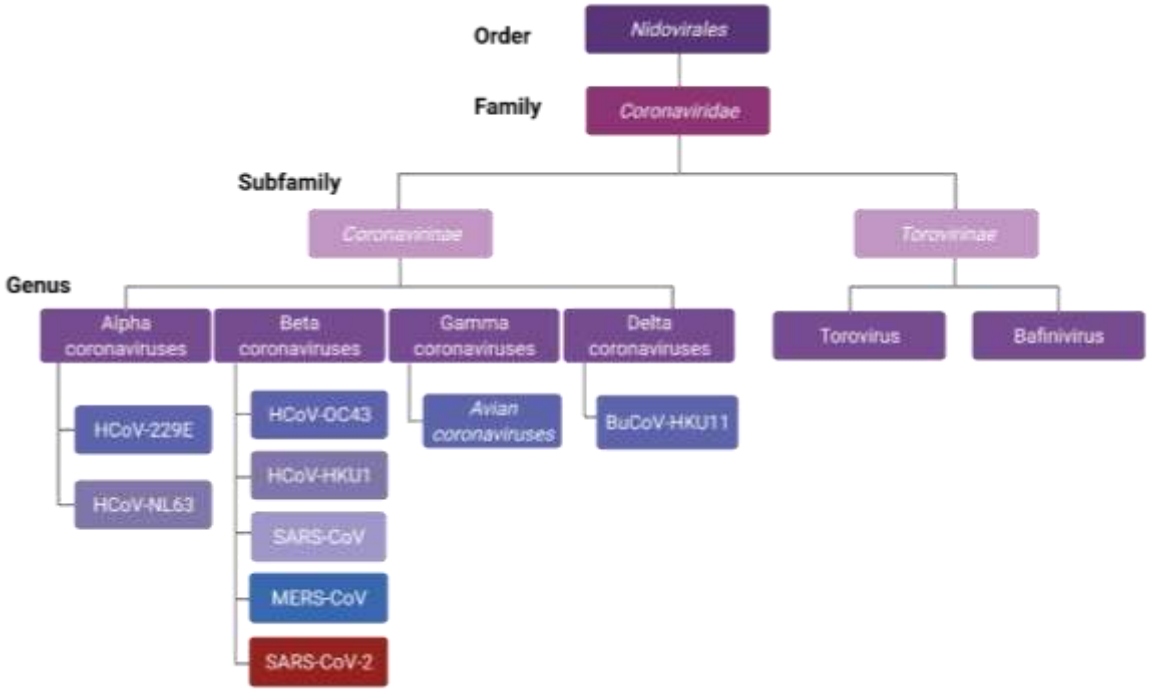

Figure 1. Classification scheme of human coronaviruses and other coronaviruses. This figure was created using BioRender.com.

2.2 SARS-CoV-2

The recently identified SARS-CoV-2, initially named the novel coronavirus 2019-nCoV, was first discovered in the city of Wuhan, China, in early December 2019 when a group of patients reported symptoms of pneumonia from an unknown cause [24]. The virus is now classified as the seventh known coronavirus to infect humans belonging to lineage B of the Betacoronavirus genus. Further, phylogenetic analysis showed that the novel coronavirus shares a sequence identity of 79% with SARS-CoV and 50% with MERS-CoV [45]. The novel SARS-CoV-2, also known as the causative agent of coronavirus disease 2019 (COVID-19), has spread all over the world in multiple waves as different virus variant, infecting more than , 470 million people and claiming the lives of over 6 million people, and thereby overwhelmingly surpassing SARS-and MERS in terms morbidity and mortality [46, 47]. In addition, the SARS-CoV-2 genome encodes four structural proteins, including the spike (S), envelope (E), membrane (M), and nucleocapsid (N) proteins (Figure 2), whereas nonstructural proteins, such as the RNA-dependent RNA polymerase, 3-chymotrypsin-like protease, and papain-like protease are encoded by the open reading frame (ORF) region [48].

Structural analysis of the S protein showed that this novel virus binds to the host cell receptor ACE2 with high affinity, mediating viral attachment and cell entry [49]. After the S protein binds to the ACE2 receptor, transmembrane serine protease 2 (TMPRSS2), an endothelial cell surface protein located on the host cell membrane, facilitates viral entry into host cells by proteolytically cleaving and activating the viral S protein [49]. Upon the virus entry into the cell, viral RNA is released, replicated, and structural proteins are synthesized, assembled, and packaged in the host cell, followed by the release of the viral particles.

In the native state, the S protein exists in a prefusion conformation as an inactive precursor; however, once it interacts with the host cell, extensive structural rearrangements of the S protein occur, allowing its fusion with the host cell membrane [49]. Further, the S protein consists of two subunits, S1 and S2, which are responsible for receptor binding and membrane fusion, respectively. The S1 subunit harbors an N-terminal domain and a receptor-binding domain (RBD). The latter domain is responsible for binding to the host cell receptor ACE2. Hence, mutations of key residues in this domain play a critical role in enhancing the interaction and binding with ACE2 [49, 50]. Also, the RBD region of the S protein is considered a primary target for protective immunity. Therefore, full S, S1, or RBD, have been considered as the major vaccine antigens since they could instigate protective immunity, specifically, NAbs that inhibit host cell binding and contamination. However, although the RBD is an interesting target for vaccines, studies have shown that its immunogenicity is weak and suggested that using the dimer form of this protein, as well as combining it with appropriate adjuvants, could provide stronger immunity. Apart from the S protein, all coronaviruses possess a smaller M glycoprotein, E protein, and N protein which is closely associated with the RNA genome. Besides providing some protection to the RNA genome, the N protein is also involved in RNA replication and transcription, whereas the E and M proteins are vital for the formation of virus particles [51].

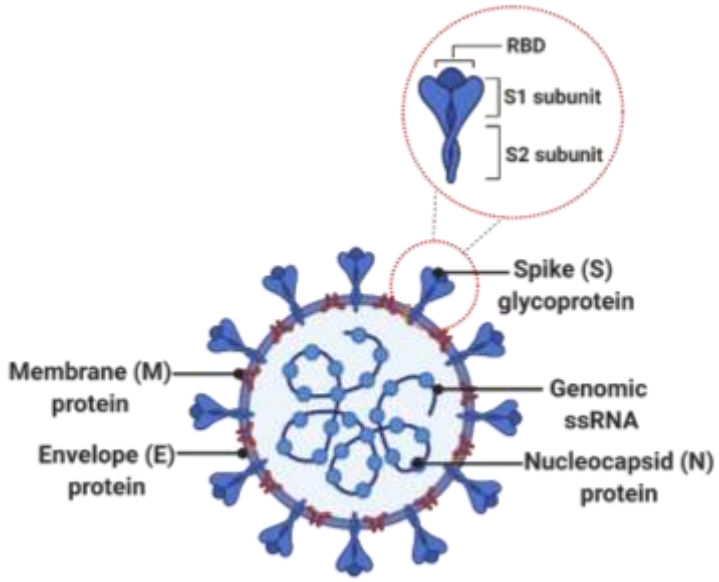

Figure 2. Schematic of SARS-CoV-2 structure. This figure was created using BioRender.com.

2.3 Overview of the immune responses to viral infections

It is well known that the immune response to viral infections is caused by an extensive array of specific and non-specific defense mechanisms. The activation of the different immune responses depends on several factors starting with pathogen recognition and antigen presentation and then followed by a cascade of immune defense mechanisms of innate and adaptive immunity.

2.3.1 Innate immune response

The innate immune system is the first line of defense. It is triggered by encountering damage-associated molecular patterns (DAMPs) released from infected tissue or dead cells or pathogen-associated molecular patterns (PAMPs), such as viral RNA and DNA [52]. Virally induced DAMPs and PAMPs stimulate tissue-resident macrophages and activate multiple innate immune pathways through Toll-like receptors (TLRs), NLRP3/inflammasome activation, or by triggering cytoplasmic

DNA sensors. This, in turn, drives the production of proinflammatory cytokines and chemokines, which subsequently leads to the stimulation of antiviral gene expression and the recruitment of more innate and adaptive immune cells for viral control and tissue hemostasis. The production of type I and type III interferons (IFNs) as a part of innate immunity initiates intracellular antiviral defense pathways while the release of IL-6 and IL-1β stimulates the recruitment of neutrophils and cytotoxic T cells [53]. Paradoxically, the dysregulated inflammatory cascade initiated by macrophages could contribute to tissue damage leading to cytokine storm as previously reported from different viral infections, including SARS-CoV-2 [52].

2.3.2 Adaptive immune response

The adaptive immune response predominately involves the interplay between both T cells and B cells which play an important role by directly killing virus-infected cells and the generation of different classes of antibodies, respectively [54]. Following the innate immune response, the adaptive immune system responds to pathogens by producing pathogen-specific humoral and cellular immunity, with T- and B- cells acting as key players. T-cell mediated immune response represents an essential arm in mediating adaptive immunity to a variety of pathogens. Pathogen peptides presented by the major histocompatibility complex (MHC) on the surface of antigen-presenting cells (APCs), such as dendritic cells (DCs), stimulate the activation, proliferation, and differentiation of naïve $CD8^+$ and $CD4^+$ T-cells. Subsequently, these cells undergo clonal expansion by interleukin-2 (IL-2) and differentiate into effector T cells in the presence of a set of cytokines engaging and activating their respective cytokine receptors [55, 56]. Importantly, achieving an effective viral clearance requires $CD8^+$ effector T cell-mediated killing of infected cells in addition to $CD4^+$ T cell-mediated enhancement of $CD8^+$ and B cell responses.

On the other hand, humoral immunity, particularly the production of NAbs, is key for combating viral infections. There is evidence that T-independent B cell responses contribute substantially to highly stable antibody repertoires, providing humoral barriers to protect against invading pathogens. However, producing humoral memory through long-lived plasma cells that produce specific antibodies of adapted avidity and function is T-cell dependent [57]. Collectively, an efficient immunological memory is achieved by the collective involvement of both T and B cells responses.

2.3.2.1 Cell-mediated immunity

Cellular immunity was previously assumed to be mediated solely by T cells; however, it is now known that several cell types are involved in the cellular immune response. Virus-infected cells can activate strong cell-mediated immune responses, which can even surpass the antibody responses during the early stages of terminating viral infections and preventing the virus from spreading within the host [54]. Cytotoxic T cells, natural killer (NK) cells, and antiviral macrophages can recognize and kill virus-infected cells. T-cells play an important role in fighting against viral infections, particularly the functional subset that expresses specific cytotoxic activity against virus-infected cells, that is, cytotoxic T cells (CTLs). These cells are presumed to prevent viral multiplication by destroying infected cells before the assembly of new virus particles. Also, helper T cells can recognize virus-infected cells producing cytokines which regulate the immune functions against the infection [1, 54].

2.3.2.2 Humoral responses

Following the recognition of the virus and/or virus-infected cells, B cells become stimulated to produce specific antibodies which can neutralize the virus by blocking its interaction with the host cell or by recognizing the antigens presented on virus-infected cells leading to the activation of NK cells via ADCC or by activating

complement-mediated lysis. While IgG antibodies are predominantly responsible for most of the antiviral activity in the serum, IgA antibodies are most important when viruses infect mucosal tissues [1, 54]. The primary function of both antibodies isotypes is blocking infection of epithelial cells, although sometimes the antibodies may transport antigen from within the body across epithelial cells to the outside. Mucosal IgA antibodies usually persists for a shorter period than IgG serum antibodies, which partly explains why immunity to mucosal pathogens is generally of much shorter duration than is immunity to systemic virus infections [54]. Despite the major role of antibodies in immune responses, not all antibodies are capable of conferring protection against viral infection. This is because not all antibodies are actually neutralizing (i.e. capable of blocking the virus attachment to host cells). Only a subset of binding antibodies can neutralize the virus by binding to its membrane receptors and preventing infection.

2.3.2.3 ADCC responses

Although NAbs are accepted as correlates of protective immunity against many viruses, they represent only a subset of the antibody repertoire that has anti-viral functions. For example, there are several antiviral functions mediated by Fc receptor binding to immune cells, including ADCC, antibody-dependent cellular phagocytosis (ADCP), antibody-dependent complement deposition (ADCD), and antibody-dependent neutrophil phagocytosis (ADNP) [58]. In ADCC, antibodies bind to viral antigens on the surface of infected target cells. Effector immune cells, most commonly NK cells, bind to the antibodies through their CD16 receptors (FcγRIII). CD16-mediated activation of NK cells results in degranulation with the release of cytotoxic molecules such as perforin and granzyme [14, 15, 17, 18, 20, 21]. NK cells, neutrophils, monocytes, and macrophages are key innate effector cells capable of

inducing ADCC *in vitro* [59]. Also, ADCC has been described for several viral infections and it has been demonstrated to be an important component of protective immunity against HIV [20], HSV [21], and influenza [14].

Furthermore, studies investigating HIV infection using rhesus macaque model have shown that antibody-mediated protection is reduced when the Fc-fraction of antibodies is cleaved [60], suggesting that Fc-mediated antiviral activity is an important additional effector function of antibodies. The presence of antibodies mediating *ex vivo* ADCC activity against the S protein in convalescent plasma from recovered COVID-19 patients has been described [58, 61]. However, less is known about the induction of functional antibodies that can mediate ADCC against the N protein, Additionally, cross-reactivity of antibodies induced by common endemic CoVs against SARS-CoV-2 has been described by few studies [62-64], which suggested that these pre-existing cross-reactive antibodies might be associated with less severe COVID-19. However, the ability of these antibodies to mediate antiviral function against SARS-CoV-2 remains poorly understood.

2.4 Dynamics of SARS-CoV-2 immune responses

Studies on SARS-CoV-2 infected patients showed that most patients mounted specific anti-SARS-CoV-2 Ab response during the acute phase of illness, some of which reported a seroconversion rate of 100% [67]. In these studies, IgM antibodies were consistently detected before IgG antibodies, peaking around the second-fifth week post-symptoms onset and then waning after another three-five weeks [67]. Similarly, IgG antibodies were reported to peak around the third-seventh week post-symptoms onset and persisted for at least eight more weeks. As for IgA, the time for seroconversion was not assessed as often as IgG and IgM, ranging between 4-24 days post symptoms onset [68, 69]. Although most studies reported an expected sequential

appearance of antibody isotypes, where IgM antibodies were detectable before IgG, this finding was not always consistent. One study reported the simultaneous detection of IgM and IgA antibodies, followed by IgG [68], whereas another reported the seroconversion of IgG in advance of IgM [70].

Moreover, NAb responses against SARS-CoV-2 have been shown to target the RBD of the S protein preferentially. Still, the levels of NAbs were variable in infected individuals and can rapidly wane over time. Therefore, other non-RBD-specific Abs, targeting the S protein, might be less efficient in terms of neutralization activity but also could have an essential role in the immune response by combining adaptive humoral responses to NK cells through the ADCC mechanism [64]. Neutralization is considered the mechanism of action for convalescent plasma therapy which has been used in COVID-19 patients and showed successful outcomes by producing good efficacy data against the disease in many small-scale studies. Further, other non-neutralizing antibody-dependent effector mechanisms such as ADCC, antibody-dependent cellular phagocytosis (ADCP), and complement-dependent cytotoxicity (CDC) are also important in protecting against infection.

2.5 COVID-19 vaccines

During the early COVID-19 pandemic, initial control measures primarily relied on social distancing, hygiene measures, repurposed drugs and achieving herd immunity through natural infection [2, 3]. However, these approaches were not very effective in hampering the virus spread across the globe. As such, since the SARS-CoV-2 genome sequence release in January 2020, all efforts have been directed towards the development of effective COVID-19 vaccines [71]. Vaccination has been long considered the cornerstone of the management of infectious diseases and a part of the multi-faceted public health response against emerging and re-emerging infectious

diseases such as influenza [72]. In the current context of COVID-19, vaccines played a critical role in defusing and controlling the pandemic. Numerous vaccine candidates have been developed based on several vaccine platforms, including the traditional ones such as inactivated and live attenuated virus vaccines and newly established ones including viral vector vaccines, DNA- and RNA-based vaccines, and recombinant subunit vaccines (Figure 3) [73]. As of March 18, 2022, more than 300 vaccine candidates have been developed, of which 149 are currently in the clinical phase of development, 195 are still in the pre-clinical phase, and 10 approved by the WHO for emergency use [74]. The vast majority of these vaccines are designed to elicit an immune response against the S protein, generating anti-S and anti-RBD binding and NAbs, but not anti-N antibodies [75].

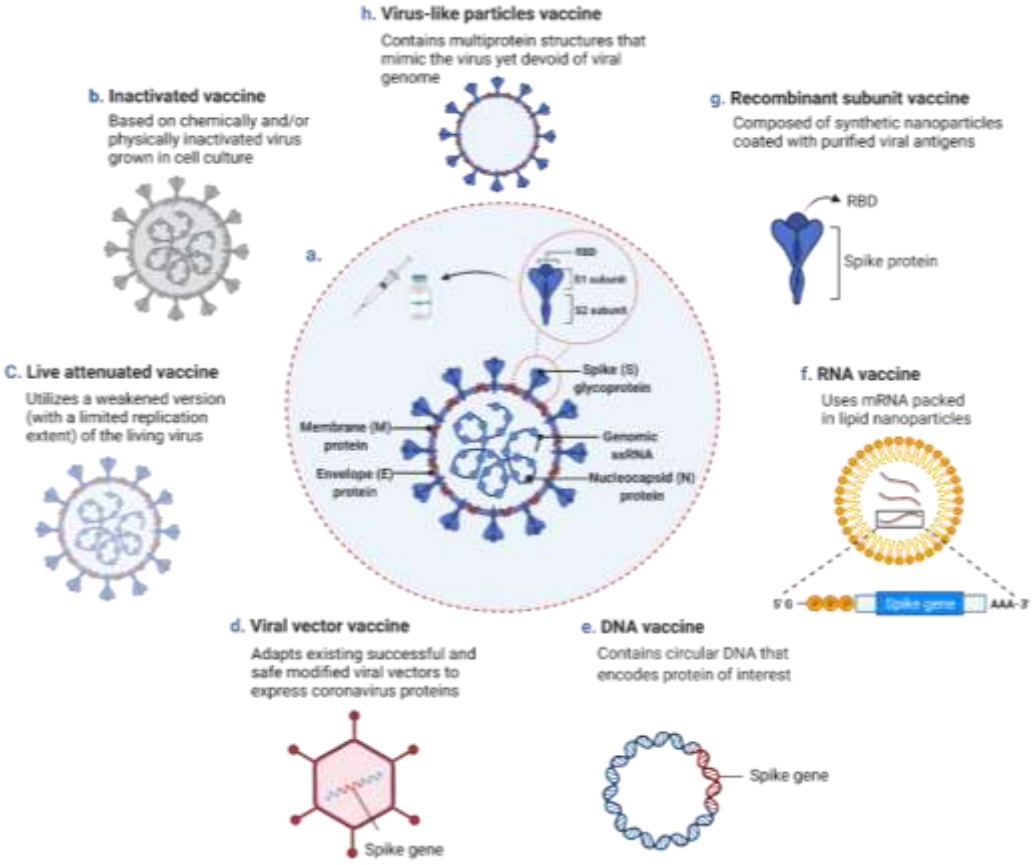

Figure 3. SARS-CoV-2 structure and contemporary COVID-19 vaccine platforms. **(a)** SARS-CoV-2 ssRNA genome and the four structural proteins. Diverse vaccine platforms include **(b)** Inactivated vaccine **(c)** Live attenuated vaccine **(d)** Viral vector vaccine **(e)** DNA vaccine **(f)** RNA vaccine **(g)** Recombinant subunit vaccine **(h)** Virus-like particles vaccine. mRNA: messenger RNA, ssRNA: single-stranded RNA, RBD: receptor-binding domain. The figure was created with BioRender.com.and published in [73].

2.6 Natural immunity-induced versus vaccine-induced immunity

Similar to natural infection, vaccines were shown to induce the production of serum IgM, IgG, and IgA [75, 76], along with durable memory B- and T-cell responses [76-78]. In addition, although immunity generated in response to natural SARS-CoV-2 infection is broader and more heterogenous, vaccine-induced immunity, especially mRNA vaccines, typically induces more consistent humoral responses with higher antibody titers [79-81]. Nevertheless, just like natural infection, this immune response may also show reduced levels in elderly and immunosuppressed individuals. High antibody titers were associated with decreased risk of symptomatic SARS-CoV-2 infection in several correlation studies. Data from phase 3 clinical trials of COVID-19 vaccines, including BNT162b2 and mRNA-1273 COVID-19 vaccines, showed a robust correlation between vaccine efficacy and high anti-S, anti-RBD, and NAbs titers, providing protection against severe disease [82, 83].

Moreover, despite the promising efficacy data of COVID-19 vaccines shown by the clinical trials, sera from mRNA-COVID-19 vaccine recipients revealed a significant reduction in neutralizing titers against several SARS-CoV-2 variants of concern (VOCs). A recent systematic review and meta-analysis indicated that the greatest

reductions in neutralizing titers were observed for the Beta variant, followed by Gamma, Delta, and Alpha which showed minimal reductions [84-86]. The majority of these reductions were accounted for E484K/Q and L452R mutations in the RBD. Of note, greater NAb titers were shown against variants following vaccination with two doses compared to a single dose [87]. Regardless, with the lack of accepted standardized antibody thresholds correlating with protection, it remains challenging to predict the effect of reduced neutralizing activity on COVID-19 vaccine effectiveness. Furthermore, since increasing evidence is suggesting that some of the newly emerging SARS-CoV-2 variants resist neutralization by antibodies induced by vaccines targeting the wild-type virus, NAbs are no longer sufficient to protect against these neutralization-resistant virus variants. Hence, other immune mechanisms might be needed to complement the available knowledge regarding protective immunity, particularly Fc-dependent effector functions which are known to induce broad immune responses [59].

CHAPTER 3: METHODOLOGY

3.1 Study design, serum samples, and ethical approval

Ethical approvals for sample collection were obtained from Qatar University (QU) institutional review board (QU-IRB # QU-IRB 804-E/17 and QU-IRB 1537-FBA/21), HMC (HMC-IRB# MRC-01-20-145, HMC-IRB# MRC-05-003, and HMC-IRB# MRC-05-007), and the Primary Health Care Corporation's Independent Review Board (Ref. No. PHCCDCR202005047).

To characterize the humoral immune responses against SARS-CoV-2, 291 convalescent sera samples were collected from previously infected COVID-19 patients during the period of SARS-CoV-2 wild-type predominance (April-August 2020) and 100 samples collected from mRNA vaccinated individuals (BNT162b2-, n=50; or mRNA-1273, n=50). and 100 samples collected from mRNA vaccinated individuals (BNT162b2-, n=50; or mRNA-1273, n=50). For the control group, 119 pre-pandemic samples collected from healthy blood donors prior to 2019 and used in previous studies [14, 88-94] were selected. The control group was used to assess the specificity of the evaluated immunoassays by including samples seropositive from various viruses such as other human coronaviruses (HCoV), non-coronavirus respiratory viruses, and non-respiratory viruses. A detailed description of all samples' characteristics is shown in Table S1 (Appendix 1).

Samples from previously infected SARS-CoV-2 patients were collected during a previous serosurvey study by the PHCC in collaboration with Dr. Gheyath Nasrallah and from a Red Crescent study conducted on a population-based sample in high exposure settings in Qatar [95, 96]. Also, samples from symptomatic COVID-19 patients were collected from the Center for Communicable Diseases (CDC) at Hamad Medical Corporation (HMC). These samples were already tested for SARS-CoV-2

antibodies using various manual and automated serological assays which have been validated before this research. Serum samples from COVID-19 vaccinated individuals were collected during another serosurvey conducted on Qatar University's community by Dr. Gheyath Nasrallah. All plasma and serum samples used in this project were separated from venous whole blood collection and stored at −80 °C until testing. Frozen samples were thawed on ice before use.

Several CE-marked *in vitro* diagnostic products were used for screening the sera samples for specific anti-SARS-CoV-2 antibodies (IgG and IgM) targeting different SARS-CoV-2 proteins, including full S protein, N protein, S1 subunit, and RBD. These assays include manual enzyme-linked immunosorbent assays (ELISA) and commercial automated immunoassays: Mindray CL900i, VIDASIII, and Abbot Architect. Also, immune response characterization was performed by detecting NAbs using ELISA-based methods and pseudovirus neutralization assay and detecting ADCC activity using commercial reporter bioassay.

3.2 Manual enzyme-linked immunosorbent assays (ELISA)

The performance of four IgM and five IgG commercial ELISA kits was evaluated for qualitatively detecting anti-SARS-CoV-2 IgG and IgM antibodies against S and N proteins in samples collected from COVID-19 patients. The selected kits were: **(i)** Epitope Diagnostic (EDI™) IgM/IgG (ref. no. KT-1033 and KT-1032), **(ii)** NovaLisa® SARS-CoV-2 IgM/IgG (ref. no. COVM0940 and COVG0940), **(iii)** AnshLabs SARS-CoV-2 IgM/IgG (ref. no. AL-1002-I and AL-1001-I), **(iv)** Diagnostic Bioprobes (DiaPro) IgG (COV19G.CE), and **(v)** Lionex COVID-19 IgM/IgG (ref. no. LIO-COV19-IgM and LIO-COV19-IgG). Further details about the kit's characteristics are shown in Table 1. All tests were carried out manually according to the manufacturers' instructions.

Table 1. Characteristics of the evaluated CE-marked ELISA kits, including the recombinant antigen used, immunoglobulin (Ig) classes, and the reported sensitivity and specificity by the company.

Assay	Manufacturer	Detected Antibody	Principle of Detection	Antigen/Antibody Coating the Plate	Reported Sensitivity	Reported Specificity
EDI™ Novel Coronavirus COVID-19 ELISA Kit	Epitope Diagnostics, Inc.	IgM	Capture ELISA	Anti-human IgM specific capture antibody	45% (vs. RT-PCR [1])	100% (vs. PCR)
		IgG	Indirect ELISA	Recombinant full length nucleocapsid protein	100% (vs. RT-PCR)	100% (vs. PCR)
NovaLisa® SARS-CoV-2 ELISA	NovaLisa Immundiagnostica GmbH	IgM	Indirect ELISA	Recombinant nucleocapsid antigen	0–30% (<11 days) 40% (≥12 days) (vs. RT-PCR)	100%
		IgG	Indirect ELISA	Recombinant nucleocapsid antigen	8–40% (<11 days) 100% (≥12 days) (vs. RT-PCR)	99.3%
AnshLabs SARS-CoV-2 ELISA	AnshLabs	IgM	Capture ELISA	Anti-human IgM specific capture antibody	100% (vs. CLIA [2]) 40% (vs. RT-PCR)	98.5% (vs. CLIA) 100% (vs. PCR)
		IgG	Indirect ELISA	Recombinant nucleocapsid and spike antigens	95% (vs. CLIA) 83.6% (vs. RT-PCR)	98.3% (vs. CLIA) 91.3% (vs. PCR)
DiaPro COVID-19 ELISA	Diagnostic Bioprobes	IgG	Indirect ELISA	Recombinant nucleocapsid and spike antigens	≥98% (vs. RT-PCR)	≥98%
Lionex COVID-19 ELISA	Lionex Diagnostics and Therapeutics	IgM	Indirect ELISA	Recombinant S1 antigen	62.5% (vs. RT-PCR)	97.9%
		IgG	Indirect ELISA	Recombinant S1 antigen	>84% (vs. RT-PCR)	99.35%

[1] RT–PCR: real-time polymerase chain reaction. [2] CLIA: chemiluminescent immunoassay.

The performance was assessed using the selected 119 pre-pandemic control sera samples and 291 sera samples collected from previously infected COVID-19 patients. The samples were categorized based on the disease status (symptomatic, n=147; or asymptomatic, n=116) and based on the time of collection following symptoms onset or positive SARS-CoV-2 RT–PCR test (≤14 days, n=119; 14-30 days, n=55; >30 days, n=117). Further details about the sample's characteristics are shown in Table 2 and Table S1 (Appendix 1).

Table 2. Characteristics of the negative control group (*n* = 119) and previously infected COVID-19 patients (*n* = 291).

	Negative Controls			**COVID-19 Patients**		
	No (%)	**Median (IQR[2])**	**Range**	**No (%)**	**Median (IQR[2])**	**Range**
Age (years)						
All	119 (100)	36.0 (15.0)	20.0–69.0	291 (100)	43.0 (21.0)	12.0–91.0
10–30	23 (19.3)			52 (17.9)		
31–60	82 (68.9)			195 (67.0)		
60+	2 (1.7)			27 (9.3)		
Gender						
Female	57 (49.6)			33 (11.3)		
Male	59 (51.3)			242 (83.2)		
Symptomatic				147 (55.9)		
Asymptomatic				116 (44.1)		
DPSO/DPD [1]						
≤14 days				119 (40.9)	8.0 (6.5)	0–14
14–30 days				55 (18.9)	19.5 (7.5)	14–30
>30 days				117 (40.2)	-	-

[1] DPSO: days post symptoms onset, DPD: days post-diagnosis; [2] IQR: interquartile range

3.3 Automated immunoassays

The performance of five CE-marked fully automated analyzers was assessed for detecting anti-SARS-CoV-2 antibodies: **(i)** VIDAS®3 SARS-CoV-2 IgG (Cat. No. 423834), **(ii)** CL-900i® SARS-CoV-2 IgG (Cat. No. SARS-CoV-2 IgG121), **(iii)** LIAISON®XL SARS-CoV-2 IgG (Cat. No. 311450), **(iv)** Architect SARS-CoV-2 IgG (Ref. 6R86-20), and **(v)** VITROS® Anti-SARS-CoV-2 Total Ab (Ref. 619 9922).

Characteristics of the assessed automated immunoassays, including detection method, targeted antigens, result interpretation, and reported sensitivity and specificity, are summarized are shown in Table 3. The performance of the immunoassays was assessed using the selected 119 pre-pandemic samples and using 107 sera samples collected from previously infected COVID-19. For this study, only samples collected after 21 days following symptoms onset or positive SARS-CoV-2 RT-PCR were included and were categorized based on the disease status (symptomatic, n=56; or asymptomatic, n=51).

Table 3. Characteristics of the automated analyzers used for anti-SARS-CoV-2 IgG detection.

Automated analyzer	Manufacturer	Detection method	Targeted antibody (ies)	Targeted antigens	Result interpretation	Reported sensitivity	Reported specificity	Reference
VIDAS®3	BioMérieux, Marcy-l'Étoile, France	ELFA	IgG	RBD of S1	< 1 AU/ml: Negative ≥ 1 AU/ml: Positive	100% (≥15 days)	98.5%	[97, 98]
CL-900i®	Mindray Bio-Medical Electronics Co., Shenzhen, China	CLIA	IgG	S and N proteins	< 10 AU/ml: Negative ≥ 10 AU/ml: Positive	100% (≥15 days)	94.9%	[99, 100]
LIAISON® XL	DiaSorin, Saluggia, Italy	CLIA	IgG	S1 and S2 proteins	< 12 AU/ml: Negative 12-15 AU/ml: Borderline > 15 AU/ml: Positive	97.5% (≥15 days)	98.2%	[98, 101]
ARCHITECT® i4000SR	Abbott Laboratories, USA	CMIA	IgG	N protein	≥1.4 S/C: Negative ≥1.4 S/C: Positive	100% (≥17 days)	99.9%	[102-104]
VITROS® ECiQ	Ortho Clinical Diagnostics, USA	CLIA	IgG, IgM, and IgA	S (S1 subunit)	<1.0 S/C: Negative ≥1.0 S/C: Positive	90.0% (≥15 days)	100%	[105]

ELFA, Enzyme-linked fluorescent assay; CLIA, chemiluminescence immunoassay; CMIA, chemiluminescent microparticle immunoassay; S: spike protein; N: nucleocapsid protein; RBD, receptor-binding domain. S1 and S2 are subunits of the spike protein; the RBD is a domain within the S1 subunit.

3.4 Surrogate virus neutralization tests (sVNT)

Two different SARS-CoV-2 surrogate virus neutralization tests (sVNT) were

assessed for the detection of NAbs that block the interaction between SARS-CoV-2 RBD and human ACE2 receptors. The first assay is an ELISA-based inhibition test developed by GenScript (Cat. No. L00847, GenScript Biotech, NJ, USA) [106-108]. This assay utilizes the same principle as ELISA using a 96-well microplate to serologically screen for NAbs targeting SARS-CoV-2 RBD (Figure 4B) [39]. Moreover, this assay was previously shown to correlate with pseudo virus neutralization test (pVNT) (R2 = 0.84) and conventional virus neutralization test (cVNT) (R2 = 0.85) [97] highly. Further, assessment validation of this assay also demonstrated high sensitivity (95.0–100%) and specificity (99.9%). According to the manufacturer's instructions, percent inhibition of ≥20% signal inhibition was considered positive (detectable NAbs), and <20% percent inhibition was considered negative (non-detectable NAbs).

The other sVNT is a novel automated immunoassay (anti-SARS-CoV-2 NTAb assay) developed by Mindray (catalog No. SARS-CoV-2 Neutralizing Antibody 121) for the quantitative detection of NAbs against SARS-CoV-2 RBD. In this assay, anti-SARS-CoV-2 NAbs in the sample competes with ACE2-ALP conjugate for RBD-binding sites (Figure 4C). The resulting chemiluminescent reaction is measured as relative light units (RLUs) by a photomultiplier built into the system, and the level of NAbs is determined via a calibration curve.

The performance of these two assays was assessed using pre-pandemic sera samples (n=70 for GenScript, n=72 for Mindray NTAb), convalescent sera collected from previously infected COVID-19 patients (n=105 for GenScript, n=74 for Mindray NTAb), and samples collected from vaccinated individuals (n=35 for GenScript, n=155 for Mindray NTAb). Samples collected from previously infected and vaccinated individuals were tested for binding IgG antibodies against SARS-CoV-2

S and N proteins using CL-900i® SARS-CoV-2 IgG test to exclude any IgG-negative samples.

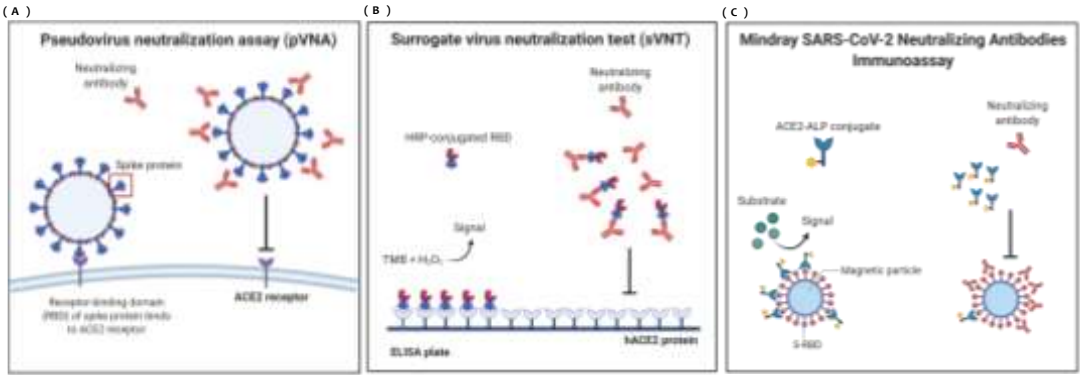

Figure 4. **Graphical illustration for the principal of three virus neutralization assays. (A)** Mechanism of pseudovirus neutralization test (pVNT) where anti-SARS-CoV-2 NAbs block the binding of SARS-CoV-2 S protein to human ACE2 receptor on the host cell surface. **(B)** Principle of GenScript surrogate virus neutralization test (sVNT) where anti-SARS-CoV-2 NAbs block the binding of HRP-conjugated RBD protein to the precoated hACE2 protein on the ELISA plate. **(C)** Principle of Mindray competitive binding NTAb immunoassay where anti-SARS-CoV-2 NAbs compete with the ACE2-ALP conjugate for RBD-binding sites on the magnetic beads. All illustrations were created using BioRender. sVNT illustration was adapted from Wang et al. [107].

3.5 Pseudovirus neutralization test (pVNT)

Pseudovirus expressing SARS-CoV-2 S protein was prepared using human embryonic kidney (HEK293T) cells (ATCC, USA) infected with vesicular stomatitis virus (VSV) ΔG-luc seed virus as previously described [109, 110]. Cells were maintained in Dulbecco's modified Eagle medium (DMEM) supplemented with 10% fetal bovine serum (FBS), 2 mM glutamine, and 1x penicillin/streptomycin in a 37 °C incubator with 5% CO_2. Briefly, the day before transfection, cells were plated into 10 cm culture

plates at a density achieving ~80% confluency. On the next day, calcium phosphate transfection reagents (Promega, USA) were used to co-transfect the cells with three plasmids (packaging plasmid pCMVΔR8.2, transducing plasmid pHR' CMV-Luc and CMV/R-SARS-CoV-2 S plasmid) and then incubated overnight. On the next day, old culture medium was replaced with fresh medium, and after 48 hours, supernatant was collected, filtered, aliquoted, and frozen at −80 °C. For the pseudovirus titration assay, HEK293T cells were used, as described by Wang et al. [110], These cells were kindly provided by Viral Pathogenesis Laboratory, Vaccine Research Center, National Institute of Health (NIH). Briefly, HEK293T cells were first plated at 1×10^4 cells per well in a 96-well white/black isoplate (PerkinElmer, MA) and cultured overnight. The following day, culture medium was removed, and two-fold serial dilutions of the pseudovirus was added to the cells and incubated for 2 hours. Then, 100µl of fresh medium was added, and after 72 hours, cells were lysed using 1x lysis buffer, and 50µl of luciferase substrate ((Bio-Glo™ Luciferase Assay System, Promega, USA) was added to each well. Luciferase activity was measured using a luminescence plate reader (Infinite pro200, Tecan).

Following pseudovirus titration, a microneutralization assay was carried out as described elsewhere and show in Figure 4A [110]. For pVNT, two-fold serially diluted sera samples were mixed and pre-incubated with 1×10^6 RLU of SARS-CoV-2 spike for 30 minutes at room temperature. Then, the mixture was added to ACE2-transfected HEK293T cells in duplicates and incubated for 2 hours, followed by adding 100µl of fresh DMEM. After 48 hours, cells were lysed, and 50µl of luciferase substrate Promega, USA) was added to each well. Luciferase activity was measured using a luminescence plate reader (Tecan, Switzerland), and percent inhibition (%) was calculated for each sample.

3.6 ADCC assay

ADCC activity was assessed using a commercial ADCC reporter bioassay kit (Promega, USA) [14, 59, 111]. ADCC effector cells (Jurkat-FcγRIIIa-NFAT-Luc, V158 high-affinity variant) were cultured in RPMI 1640 medium (Gibco, USA) with 10% FBS, 1 mM sodium pyruvate, and 1x penicillin/streptomycin at 37 °C in a humidified CO2 incubator and passaged every 2–3 days. This assay measures the ability of serum antibodies to activate the NFAT (nuclear factor of activated T cells) pathway through FcγRIII (the pathway that initiates ADCC in NK cells) in the presence of target antigens coated on a 96-well plate. ADCC protocol is summarized in Figure 5 below. Briefly, 96-well plates were coated overnight at 4ºC with purified SARS-CoV-2 spike (SinoBiological, USA, Cat No.# 40589-V08B10) and nucleocapsid (SinoBiological, USA, Cat No.# 40588-V08B) antigens (300 ng/well and 100 ng/well, respectively) in 1x PBS. Wells were washed with PBS in 0.05% Tween20 to remove unbound proteins and then blocked with 5% bovine serum albumin (BSA). Then, heat-inactivated sera were serially diluted (in blocking buffer), added, and incubated at 37°C for 2 hours. ADCC effector cells were then added to each well (75,000 cells/well) and incubated overnight at 37°C. After incubation, a luciferase reagent (Bio-Glo) was used to measure luminescence activity using a luminescence plate reader. ADCC activity was reported as fold induction in the relative light units (RLUs) which was calculated as follows: Fold of induction = RLU of induced/RLU of no serum control.

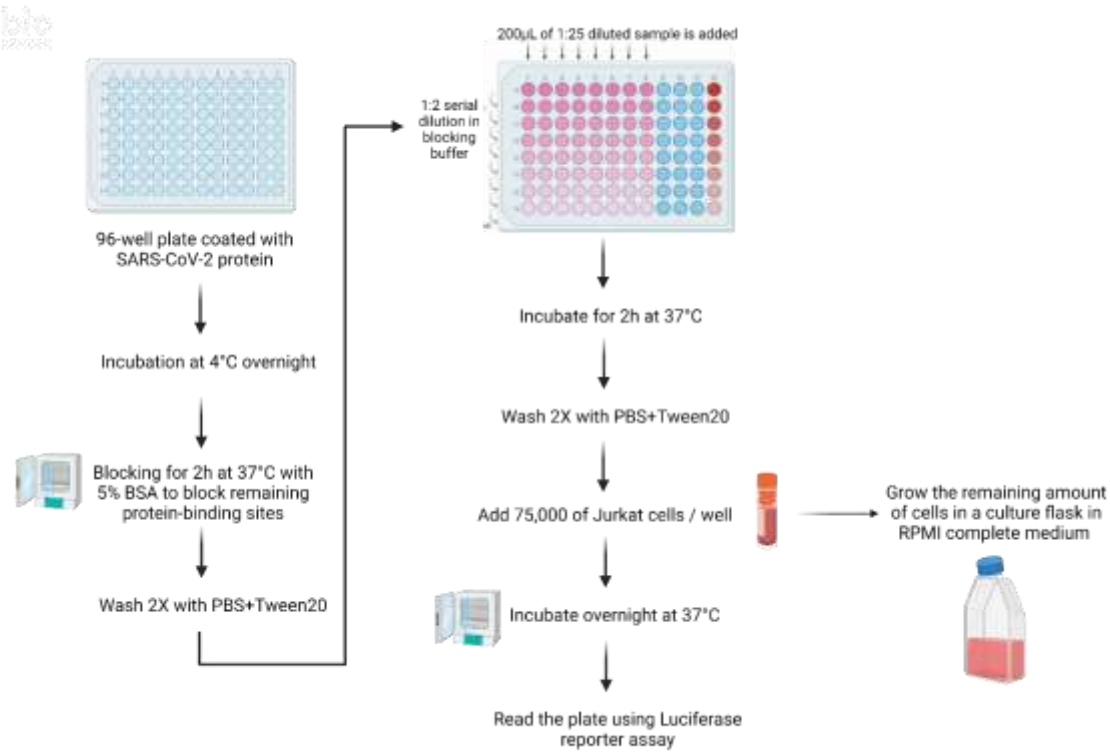

Figure 5. Graphical illustration of ADCC assay protocol. This figure was created using BioRender.com.

3.7 Statistical analysis

To assess the performance of each selected assay, sensitivity, specificity, overall agreement, positive predictive value, negative predictive value, and Cohen's kappa statistic were calculated. Informed by literature, borderline results were considered positives for all manual and automated assays [27, 28]. Concordance assessment between the assays was done by calculating the overall, positive, and negative percent agreement, as well as Cohen's kappa coefficient (κ) which is a robust statistical measure of agreement used to test inter-rater reliability and estimate the level of agreement (beyond chance) between two diagnostic tests. Ranging between 0 and 1, a kappa value ≤0.40 denotes poor agreement, a value between 0.40 and 0.75 denotes fair/good agreement, and a value ≥0.75 denotes excellent agreement [112]. Data are

presented as mean ± standard error mean (SEM). Group differences were evaluated using one-way analysis of variance (ANOVA), and Kruskal–Wallis test, followed by Dunn's post hoc tests. Chi-square was used to assess the significance between overall sensitivities and specificities.

In addition, correlation, and linear regression analyses were performed to assess the correlation between the assays and between the different humoral immune responses. Non-parametric Spearman's correlation coefficient (ρ) and Pearson correlation coefficient (r) were calculated to assess the correlation: a coefficient of <0.3 indicates no or negligible correlation, 0.3–0.5 is a weak correlation, 0.5–0.7 is a moderate correlation, 0.7–0.9 is a strong correlation, and >0.9 is a very strong correlation [113]. Significant differences were represented as: * $p < 0.05$; ** $p < 0.01$; *** $p < 0.001$; **** $p < 0.0001$. The significance level was set at 5%, and 95% confidence intervals (CI) were reported. Receiving operating characteristic (ROC) curve analysis and Youden index were used to study the diagnostic performance of each assay and assess the assays thresholds (cutoff) by identifying optimized ones. A nonparametric ROC analysis was performed for each automated immunoassay to estimate the area under the curve (AUC). Statistically, the bigger the AUC, the more accurate a tool in terms of diagnostic performance. The relation between AUC and diagnostic accuracy applies as follows: an AUC of <0.5 suggests no discrimination (ability to diagnose patients with and without the disease or condition based on the test), 0.5–0.6 indicates poor discrimination, 0.6–0.7 indicates sufficient discrimination, 0.7–0.8 is considered good, 0.8–0.9 is excellent, and >0.9 is outstanding [114, 115]. The cut-off values for optimal sensitivity and specificity were determined by calculating Youden's index J using the formula: J = sensitivity + specificity − 1. This index is typically used as a summary measure of ROC curve to help determine the optimal thresholds for each

assay and to compare it with other tests [116].

Moreover, NAbs titers and ADCC activity were correlated with different SARS-CoV-2 antibody isotypes (IgG and IgM) to identify antibodies that best correlate with the presence of these responses and perhaps predict protective immunity in infected and vaccinated individuals. For NAbs and ADCC activity, each sera sample was tested in duplicates. All statistical analyses were performed using Microsoft Excel 2016 and GraphPad Prism Version 9.0 (GraphPad, California, USA).

CHAPTER 4: RESULTS

4.1 Performance evaluation of manual IgM ELISA kits

The performance assessment of the four IgM ELISA kits is summarized in Figure 6-10, Table 4, and Table S2 (Appendix 2).

4.1.1 Performance assessment in symptomatic and asymptomatic COVID-19 patients

Figure 6 and Table S2 (Appendix 2) summarize the performance assessment of each IgM ELISA kit in symptomatic and asymptomatic COVID-19 patients. The highest sensitivity values were observed in samples collected from symptomatic patients by all ELISA kits where Lionex showed the highest sensitivity at 75.5% (95% CI: 68.6–82.5), followed by AnshLabs at 57.1% (95% CI: 49.1–65.1), EDI at 52.4% (95% CI: 44.3–60.5), and NovaLisa at 45.6% (95% CI: 37.5–53.6). In samples collected from asymptomatic COVID-19 patients, the sensitivity was highest in Lionex ELISA (39.7%; 95% CI: 30.8–48.6) and lowest in AnshLabs (3.4%; 95% CI: 0.13–6.8). In addition, the point distribution of calculated index values for each IgM ELISA is shown in Figure 7. The highest index values were obtained by samples collected from symptomatic COVID-19 patients compared to asymptomatic patients by all kits. The clearest separation of known positive and known negative samples was shown by EDI (Figure 7A).

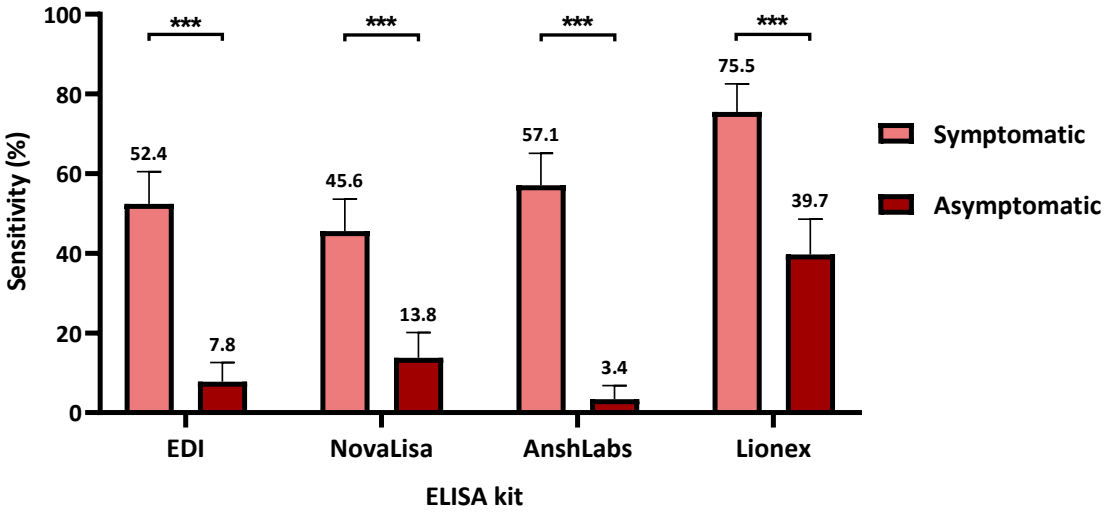

Figure 6. IgM ELISA sensitivity according to COVID-19 status (symptomatic or asymptomatic). Chi-square was used to calculate the significance between the sensitivities in symptomatic and asymptomatic patients for each kit, ***p<0.001. Please note that these results were published in [117].

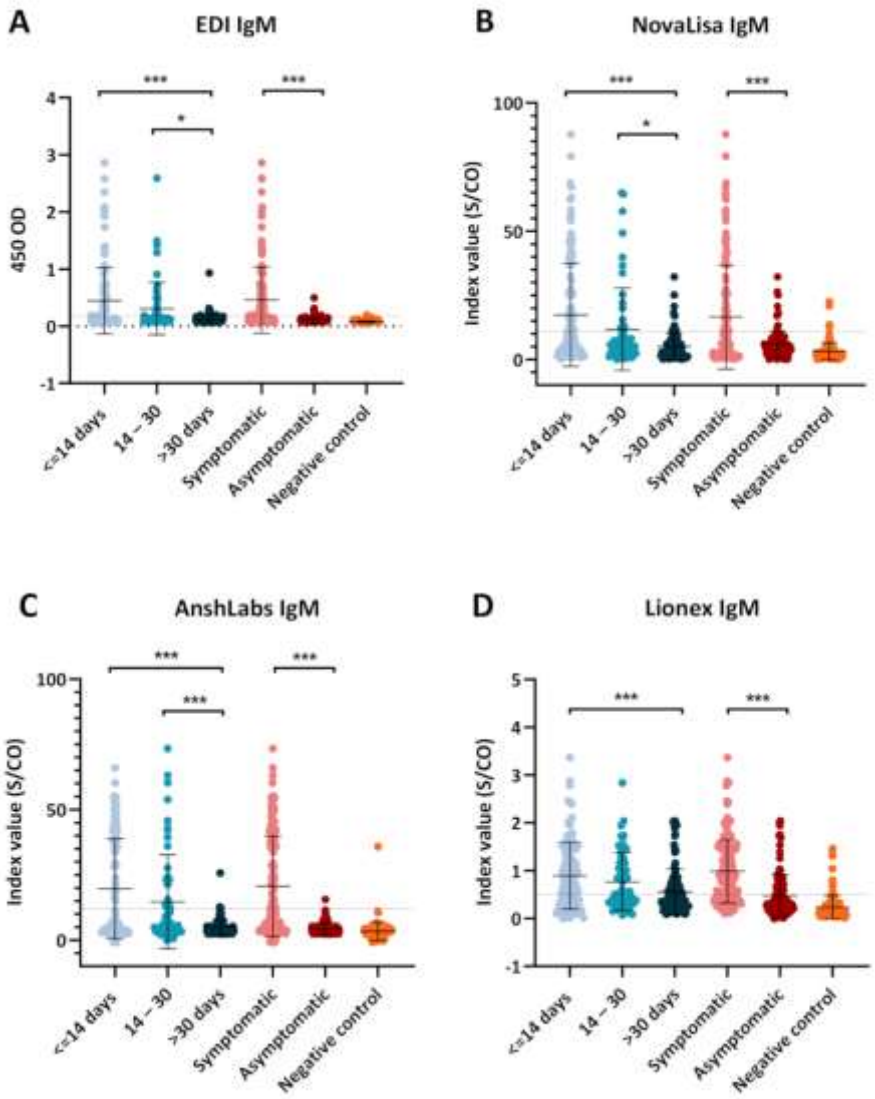

Figure 7. Dot plot distribution of the IgM ELISA index values according to the different time points of sampling (≤14, 14–30, >30 days) and coronavirus disease 2019 (COVID-19) patient classification (symptomatic or asymptomatic). Each dot plot represents the index values obtained with each serological assay: (**A**) EDI™, (**B**) NovaLisa, (**C**) AnshLabs, and (**D**) Lionex. Results are expressed as a ratio of the sample signal to the cutoff for all tests except the EDI™ assay, which is expressed in optical density. One-way analysis of variance (ANOVA) was used to compare the differences between groups, *p<0.05, ***p<0.001. Please note that these results were published in [117].

4.1.2 Performance assessment of samples collected at different time intervals in infected patients

The performance assessment of each IgM ELISA kit at the three-time intervals of sample collection post symptoms onset or positive SARS-CoV-2 RT–PCR test (≤14, 14–30, >30 days) is summarized in Figure 8 and Table S2 (Appendix 2). The sensitivity significantly decreased over time, where the highest values were shown in samples collected before 14 days ranging from 48.7% (95% CI: 39.8–57.7) for EDI to 66.4% (95% CI: 57.9–74.9) for Lionex. In samples collected within the second time interval (14–30 days), the sensitivity was lowest for NovaLisa (29.1%, 95% CI: 17.1-41.1) but remained relatively high for Lionex (61.8%, 95% CI: 49.0-74.7). After 30 days of sampling, the lowest sensitivity was shown by AnshLabs (6.8%, 95% CI: 2.3-11.4) and highest by Lionex (47.9%, 95% CI: 38.8-56.9). Since most of the samples at the third time interval were collected from asymptomatic patients, the sensitivity was re-adjusted and calculated using samples collected from symptomatic patients only to obtain a more accurate estimation. As shown in Figure 9, the sensitivity increased by all ELISA kits at the first-time interval (≤14 days), ranging from 62.4% for NovaLisa to 85.9% for Lionex. The sensitivity was also relatively higher in the second time interval, ranging from 54.2% for NovaLisa to 75.0% for Lionex. Nevertheless, the sensitivity was significantly lower at the third time interval for all kits, ranging from 2.6% for NovaLisa to 52.6% for Lionex. Similarly, the dot plot distribution of the index values at the three-time interval showed a significant decrease over time by all kits (Figure 7). Further, the most evident separation between different time intervals of sample collection was obtained by NovaLisa (Figure 7B).

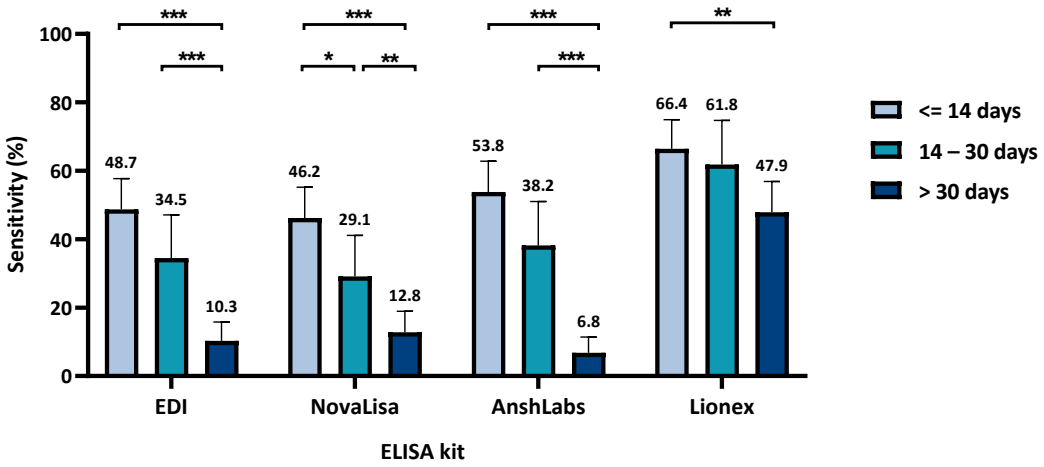

Figure 8. IgM ELISA sensitivity according to time of sample collection after symptoms onset or positive severe acute respiratory syndrome coronavirus 2 (SARS-CoV-2) RT-PCR for both symptomatic and asymptomatic patients. Chi-squared test was used to detect the presence of a statistically significant difference in the sensitivity between the time intervals for each assay, *p<0.05, **p<0.01, ***p<0.001. Please note that these results were published in [117].

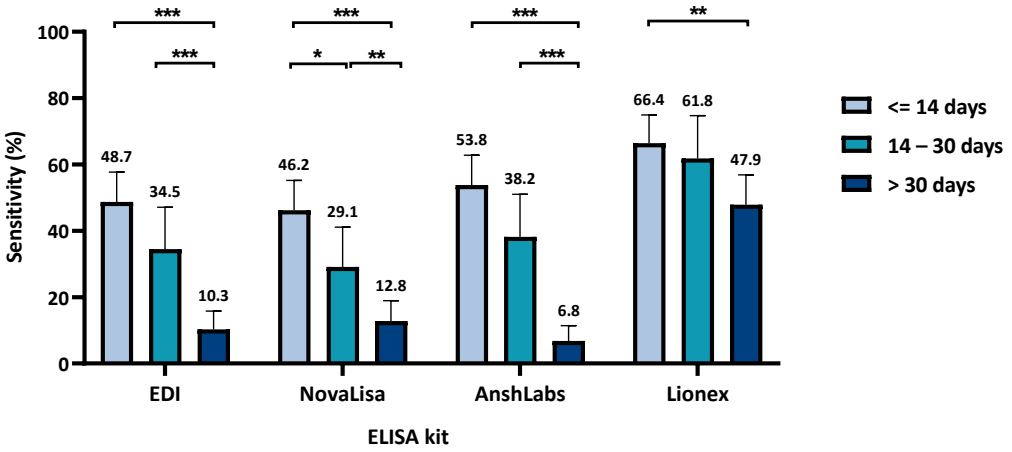

Figure 9. IgM ELISA sensitivity according to time of sampling after symptoms onset from only symptomatic coronavirus disease 2019 (COVID-19) patients. Chi-square test was used to detect the presence of a statistically significant difference in the sensitivity between the time intervals in each assay. *p<0.05, **p<0.01, ***p<0.001. Please note that these results were published in [117].

4.1.3 Specificity assessment

Table 4 summarizes the overall specificity of the IgM ELISA kits for each control subgroup. The highest overall specificity was shown by EDI at 99.2% (95% CI: 97.5–100) and the lowest specificity was shown by Lionex at 88.2% (96% CI: 82.4–92.0) due to cross-reactivity with other HCoVs, non-CoV respiratory viruses and non-respiratory viruses.

4.1.4 Agreement between IgM ELISA Kits

Pairwise correlation between IgM ELISA showed the best overall agreement between EDI and NovaLisa (90.7%, 95% CI: 87.4–94.1) with a kappa index of 0.784, indicating an excellent agreement (Figure 10A). Also, a very good agreement was observed between AnshLabs and EDI along with AnshLabs and NovaLisa [85.2%, 95% CI: 81.1–89.3), k = 0.649 and 84.2% (95% CI: 80.0–88.4), k = 628, respectively]. In samples collected during the first time-interval (≤14 days), EDI and Lionex showed the best agreement at 90.8% (95% CI: 85.6–96.0) with a kappa index of 0.815 (Figure 10B). However, in the second time-interval (14–30 days), EDI and AnshLabs showed the best agreement at 96.4% (95% CI: 91.4–100) with a kappa index of 0.922 (Figure 10C). In the third time interval (>30 days), EDI and AnshLabs also showed the best agreement at 88.9% (95% CI: 83.2–94.6) with a kappa index of 0.260 (Figure 10D). Additionally, in samples collected from symptomatic COVID-19 patients, EDI and AnshLabs demonstrated the best agreement at 88.4% (95% CI: 83.3–93.6) with a kappa index of 0.767, indicating an excellent agreement (Figure 10E). Also, EDI and AnshLabs showed the best agreement in samples collected from asymptomatic individuals at 92.2% (95% CI: 87.4–97.1), but the kappa index was low at 0.273 (Figure 10F).

Table 4: Specificity of the four evaluated IgM ELISA kits.

		Specificity (%, 95% confidence interval)			
Subgroup with IgM antibodies against	**No. of samples**	**EDI**	**AnshLabs**	**NovaTec**	**Lionex**
Other coronaviruses (SARS-CoV, MERS-CoV, HCoV-229E, NL63, OC43, and HKU1)	20	20/20 (**100%**)	17/20 (**85.0%**)	20/20 (**100%**)	15/20 (**75.0%**)
Non-CoV respiratory viruses (Influenza and RSV)	28	28/28 (**100%**)	27/28 (**96.4%**)	25/28 (**89.3%**)	26/28 (**92.9%**)
Non-respiratory viruses (HEV, HGV, HCV, HBV, DENV, WNV, CHIKV, B19, HSV-1, HSV-2, EBV, HHV-6, and HHV-8)	65	64/65 (**98.5%**)	62/65 (**95.4%**)	62/65 (**95.4%**)	59/65 (**90.8%**)
Antinuclear antibodies (ANAs)	6	6/6 (**100%**)	6/6 (**100%**)	6/6 (**100%**)	5/6 (**83.3%**)
Overall specificity	119	**99.2%** (118/119:97.5–100)	**95.0%** (113/119:91.0–98.9)	**89.1%** (106/119:83.5–94.7)	**88.2%** (105/119:82.4–92.0)

MERS: Middle East respiratory syndrome coronavirus, SARS-CoV: severe acute respiratory syndrome coronavirus, RSV: respiratory syncytial virus, HSV-1: herpes simplex virus 1, HSV-2 herpes simplex virus 2, HHV-6: human herpesvirus-6, HHV-8: human herpesvirus-8, EBV: Epstein–Barr virus, HBV: hepatitis B virus, HCV: hepatitis C virus, HEV: hepatitis E virus, HGV: hepatitis G virus, B19: parvovirus B19, WNV: West Nile virus Please note that these results were published in [117].

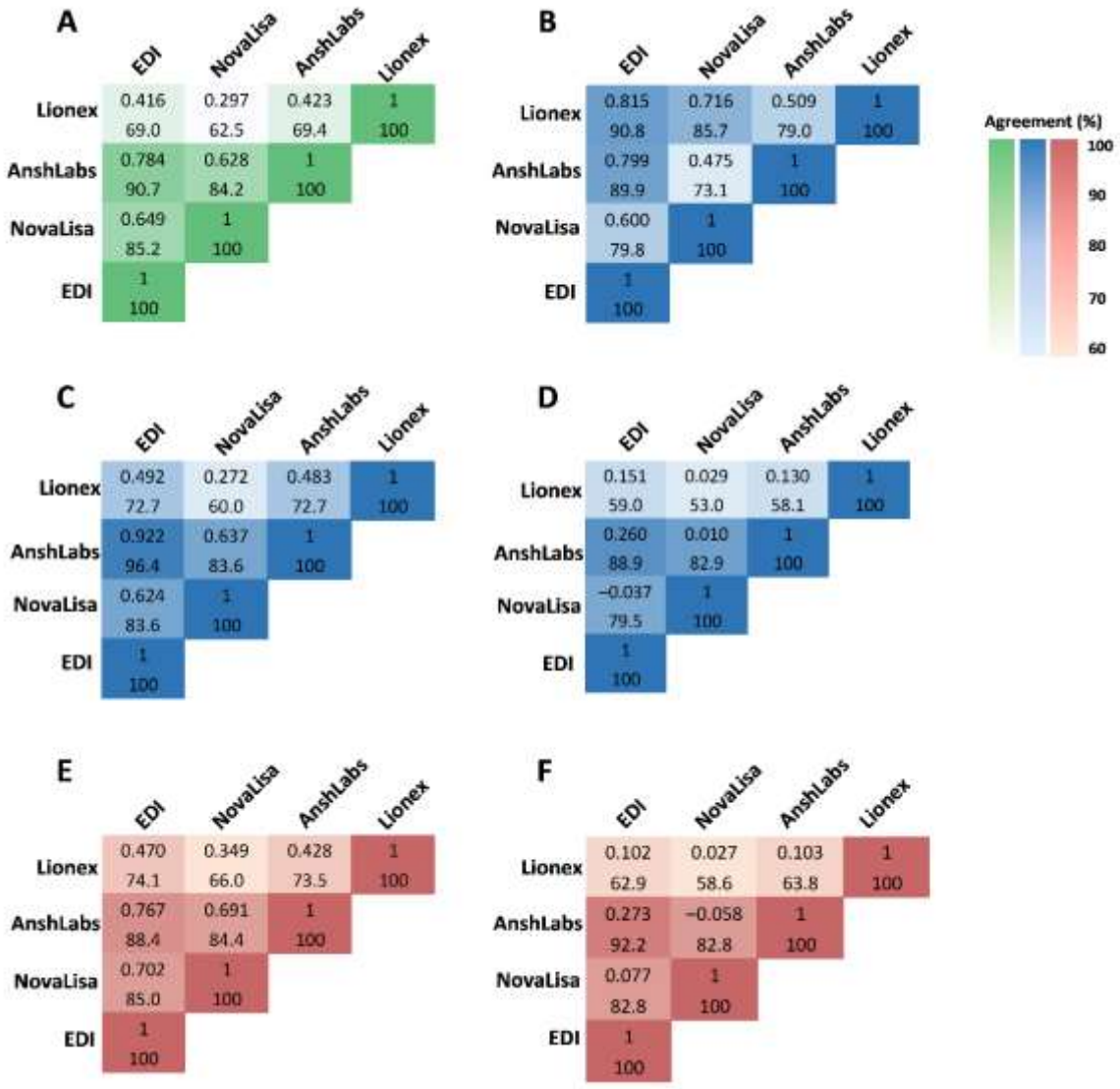

Figure 10. Concordance assessment for the overall agreement and kappa (k) among all IgM ELISA tests. (**A**) The overall agreement, (**B**) agreement in samples collected ≤14 DPSO/DPD, (**C**) agreement in samples collected 14–30 DPSO/DPD, (**D**) agreement in samples collected >30 DPSO/DPD, (**E**) agreement in samples collected from symptomatic coronavirus disease 2019 (COVID-19) patients, (**F**) agreement in samples collected from asymptomatic COVID-19 patients. Please note that these results were published in [117].

4.2 Performance evaluation of manual IgG ELISA kits

The performance assessment of the five IgG ELISA kits is summarized in Figure 11-14, Table 5, and Table S2 (Appendix 2).

4.2.1 Performance assessment in symptomatic and asymptomatic COVID-19 patients

Figure 11 and Table S2 (Appendix 2) show the performance assessment of each IgG ELISA kit in symptomatic and asymptomatic COVID-19 patients. Samples collected from symptomatic patients showed significantly higher sensitivity by all kits where the highest values were demonstrated by AnshLabs at 89.1% (95% CI: 84.1–94.2), followed by both NovaLisa and Lionex at 84.1% (95% CI: 77.9–90.3), then EDI at 71.4% (95% CI: 64.1–78.7), and DiaPro at 67.3% (95% CI: 59.8–74.9). In asymptomatic patients, the sensitivity ranged from 24.3% (95% CI: 14.2–34.3) to 86.2% (96% CI: 79.9–92.5) for DiaPro and AnshLabs, respectively. Further, the point distribution of calculated index values is shown in Figure 12. Again, significantly higher index values were observed in symptomatic patients compared to asymptomatic patients by NovaLisa, DiaPro, and AnshLabs (Figure 12B-D).

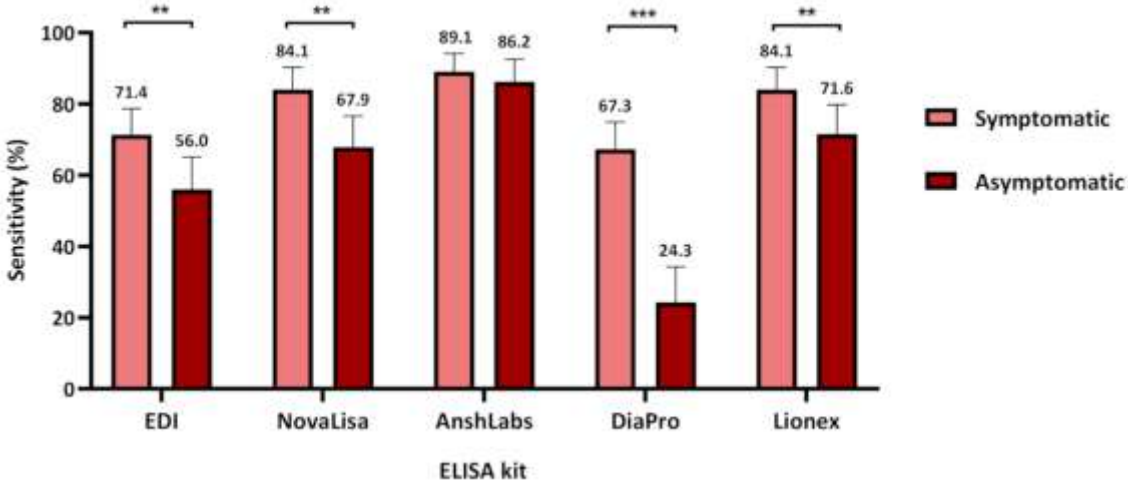

Figure 11. IgG ELISA sensitivity according to coronavirus disease 2019 COVID-19 classification (symptomatic or asymptomatic). Chi-square was used to calculate the

significance between the sensitivities in symptomatic and asymptomatic patients for each assay, $^{**}p < 0.01$, $^{***}p < 0.001$. Please note that these results were published in [117].

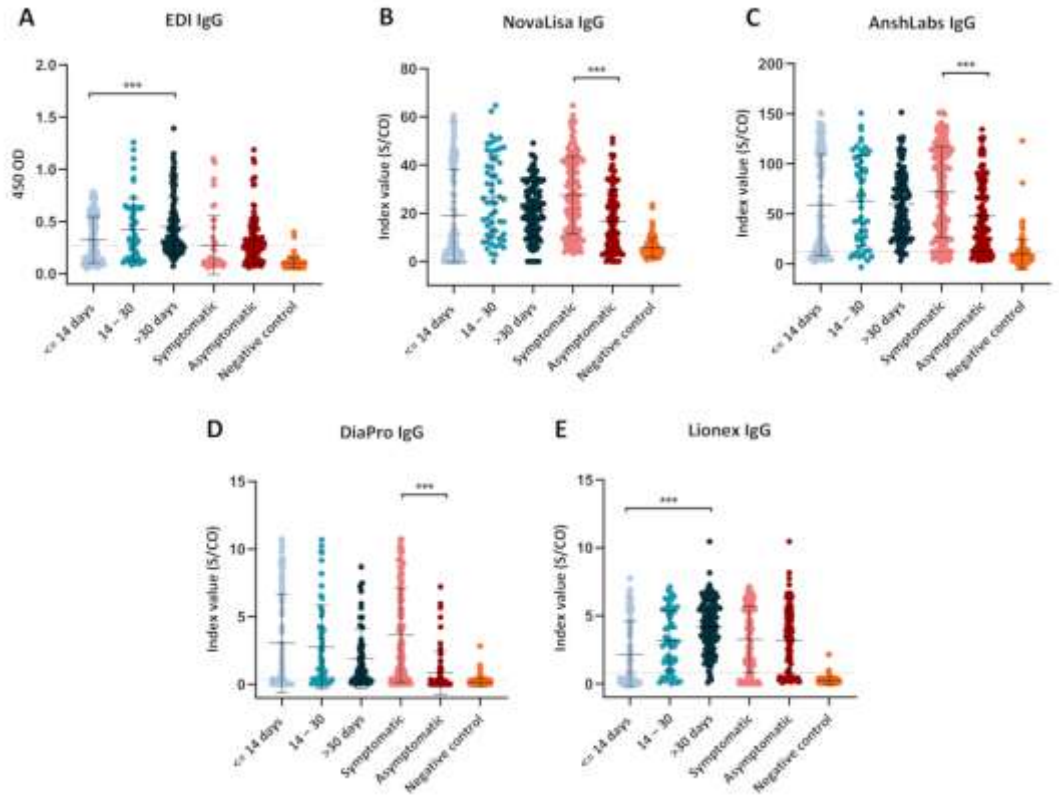

Figure 12. Dot plot distribution of the IgG ELISA index values according to the different time points of sampling (≤14, 14–30, >30 days) and coronavirus disease 2019 (COVID-19) patient classification (symptomatic or asymptomatic). Each dot plot represents the index values obtained with each serological assay: **(A)** EDI™, **(B)** NovaLisa, **(C)** AnshLabs, **(D)** DiaPro, and **(E)** Lionex. Results are expressed as a ratio of the sample signal to the cutoff for all tests except the EDI™ assay, which is expressed in optical density. One-way analysis of variance (ANOVA) was used to compare the differences between groups, $^{***}p<0.001$. Please note that these results were published in [117].

4.2.2 Performance assessment of samples collected at different time intervals in infected patients

The performance assessment of the five IgG ELISA kits in the three-time intervals is summarized in Figure 13 and Table S2 (Appendix 2). The lowest sensitivities were seen in samples collected within less than 14 days by all kits ranging between 48.7% (95% CI: 39.8–57.7) for DiaPro and 78.2% (95% CI: 70.7–85.6) for AnshLabs. After the second week of sampling (14-30 days), the sensitivities of all kits increased, peaking at 83.6% (95% CI: 73.9–93.4) for AnshLabs. Following one month of sampling, the sensitivities significantly increased by all kits, except DiaPro, dropping to 53.5% (95% CI: 41.9–65.1). Both AnshLabs and Lionex demonstrated sensitivities above 95% after one month of sampling (95.7% and 96.6%, respectively). The dot plot distribution of the index values at the three-time interval showed a significant increase in index values between the first (≤14 days) and third (>30 days) time intervals by both EDI and Lionex (Figure 12A, E).

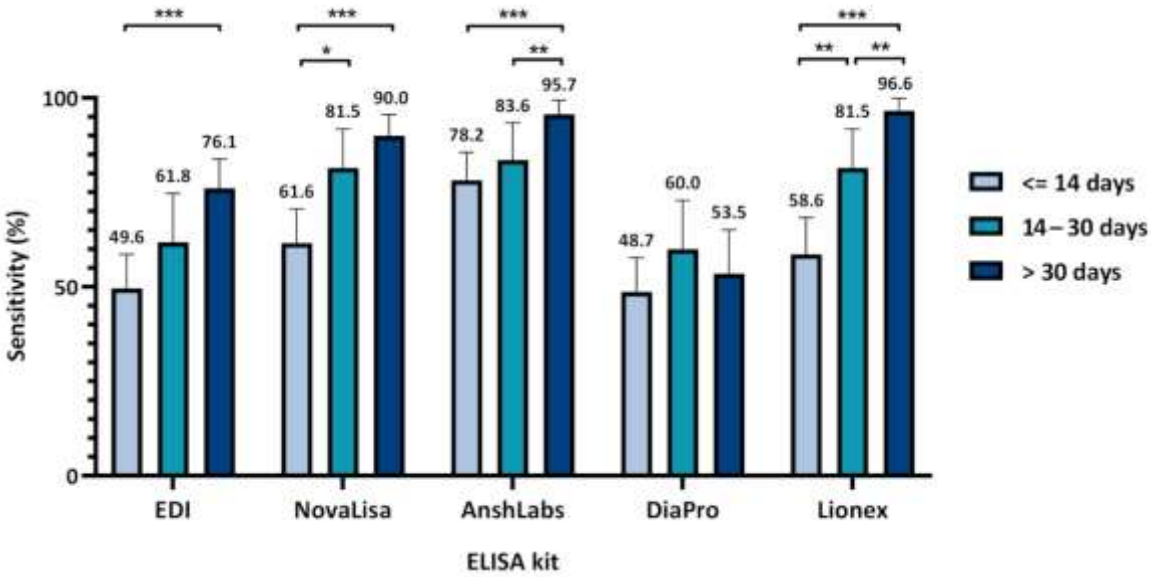

Figure 13. Assays sensitivity according to time of sampling after symptoms onset or positive severe acute respiratory syndrome coronavirus 2 (SARS-CoV-2) RT–PCR test. Chi-squared test was used to detect the presence of a statistically significant difference

in the sensitivity between the time intervals for each assay *p< 0.05, **p< 0.01, *** p<0.001. Please note that these results were published in [117].

4.2.3 Specificity and cross-reactivity assessment

Table 5 summarizes the overall specificity for IgG ELISA kits which ranged from 88.2% (95% CI: 82.4–92.0) to 99.2% (95% CI: 97.5–100). When assessing the specificity by each control subgroup, EDI showed the highest specificity in all subgroups, cross-reacting with only one sample seropositive for antibodies against influenza (98.5%).

4.2.4 Agreement between IgG ELISA Kits

Pairwise correlation between the five IgG ELISA kits showed that EDI and DiaPro have the best overall agreement at 87.8% (95% CI: 83.7–91.9) with k= 0.753, indicating an excellent agreement (Figure 14A). Also, NovaLisa and Lionex pair as well as NovaLisa and AnshLabs pair showed a very good agreement at 87.1% (95% CI: 83.0–91.1), k = 0.619 and 86.3% (95% CI: 82.2–90.5), k = 0.540, respectively. In samples collected during the first time-interval (≤14 days), EDI and DiaPro had the best agreement at 94.1% (95% CI: 89.9–98.3) with k= 0.882, indicating an excellent agreement (Figure 14B). EDI and DiaPro pair also showed the best agreement within the second time-interval (14-39 days) [90.9% (95% CI: 83.3–98.5), k= 0.809] as shown in Figure 14C. In the third time-interval (>30 days), the best agreement was denoted by Lionex with NovaLisa, DiaPro, and AnshLabs at 93.6% (95% CI: 89.1–98.2), 97.4% (95% CI: 94.6–100), and 94.4% (95% CI: 89.0–99.7), respectively (Figure 14D). Moreover, when comparing the agreement between samples collected from symptomatic and asymptomatic COVID-19 patients, NovaLisa and AnshLabs showed the best agreement in the symptomatic group at 93.2% (95% CI: 88.9–97.5)

with k= 0.718, indicating a very good agreement (Figure 14E), whereas NovaLisa and Lionex showed the best agreement in the asymptomatic group at 87.2% (95% CI: 80.9–93.4) with k= 0.701 (Figure 14F).

Table 5: Specificity of the four evaluated IgG ELISA kits.

Control Subgroup	No. of Samples	IgG ELISA				
		EDI	**NovaLisa**	**AnshLabs**	**DiaPro**	**Lionex**
Other coronaviruses (SARS-CoV, MERS-CoV, HCoV-229E, NL63, OC43, and HKU1)	20	19/20 (**95.0%**)	17/20 (**85.0%**)	17/20 (**85.0%**)	19/20 (**95.0%**)	20/20 (**100%**)
Non-CoV respiratory viruses (H1N1 influenza and RSV)	28	28/28 (**100%**)	19/28 (**67.9%**)	14/28 (**50.0%**)	26/28 (**92.9%**)	27/28 (**96.4%**)
Non-respiratory viruses (HEV, HGV, HCV, HBV, DENV, WNV, CHIKV, B19, HSV-1, HSV-2, EBV, HHV-6, and HHV-8)	65	64/65 (**98.5%**)	58/65 (**89.2%**)	54/65 (**83.1%**)	64/65 (**98.5%**)	63/65 (**96.9%**)
Antinuclear antibodies (ANAs)	6	6/6 (**100%**)	6/6 (**100%**)	5/6 (**83.3%**)	6/6 (**100%**)	6/6 (**100%**)
Overall Specificity	119	**98.3%** (117/119:96.0–100)	**96.6%** (115/119:93.4–99.9)	**84.0%** (100/119:77.5–90.6)	**75.6%** (90/119:67.9–83.3)	**97.5%** (116/119:94.7–100)

MERS: Middle East respiratory syndrome coronavirus, SARS-CoV: severe acute respiratory syndrome coronavirus, RSV: respiratory syncytial virus, HSV-1: herpes simplex virus 1, HSV-2 herpes simplex virus 2, HHV-6: human herpesvirus-6, HHV-8: human herpesvirus-8, EBV: Epstein–Barr virus, HBV: hepatitis B virus, HCV: hepatitis C virus, HEV: hepatitis E virus, HGV: hepatitis G virus, B19: parvovirus B19, WNV: West Nile virus. Please note that these results were published in [117].

Additionally, in samples collected from symptomatic COVID-19 patients, EDI and AnshLabs demonstrated the best agreement at 88.4% (95% CI: 83.3–93.6) with a kappa index of 0.767, indicating an excellent agreement (Figure 12E). Also, EDI and AnshLabs showed the best agreement in samples collected from asymptomatic individulas at 92.2% (95% CI: 87.4–97.1), but the kappa index was low at 0.273 (Figure 12F). Further details about the findings of this study can be found in [117].

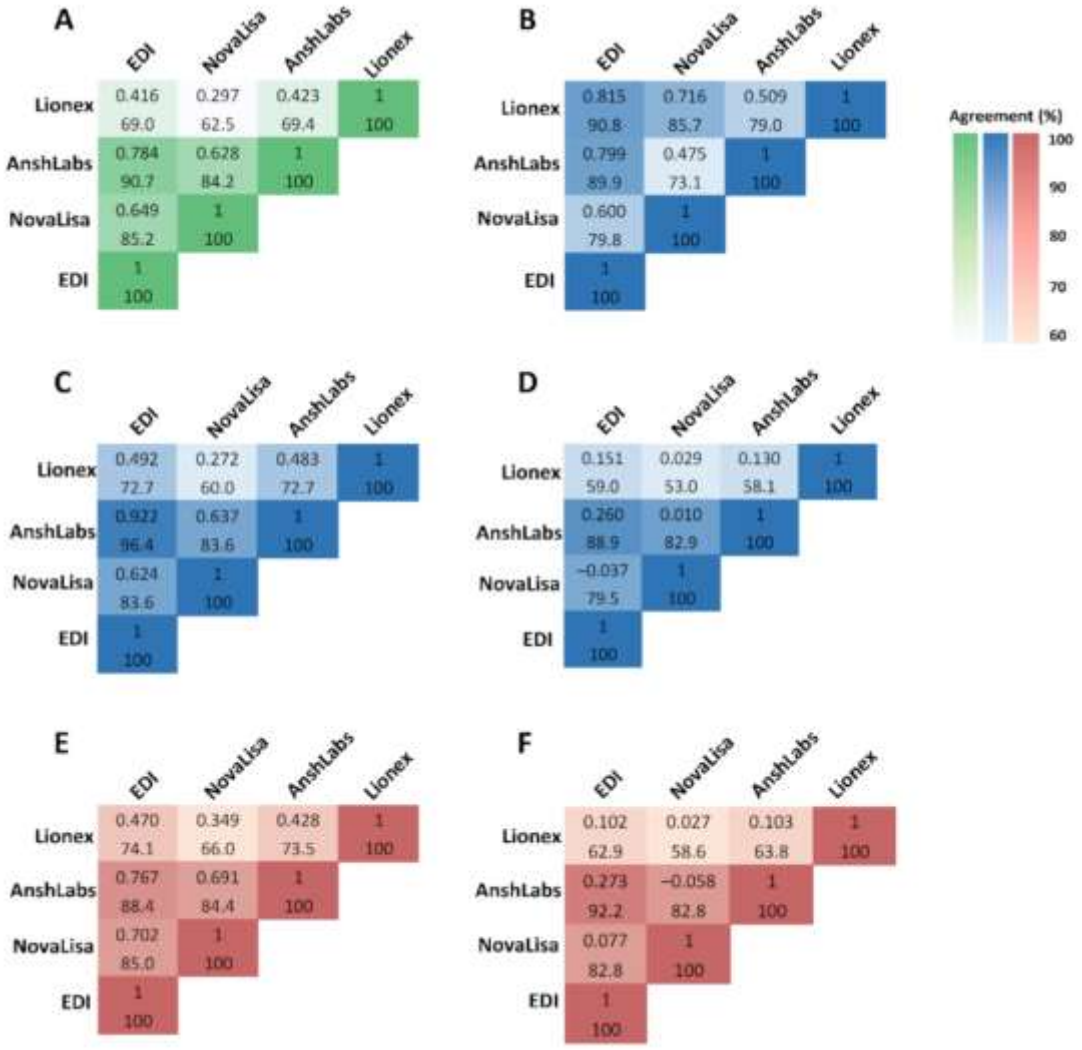

Figure 14. Concordance assessment for the overall agreement and kappa (k) among all IgM ELISA tests. **(A)** The overall agreement, **(B)** agreement in samples collected ≤14 DPSO/DPD, **(C)** agreement in samples collected 14–30 DPSO/DPD, (D) agreement in samples collected >30 DPSO/DPD, **(E)** agreement in samples collected from COVID-

19 patients, **(F)** agreement in samples collected from asymptomatic COVID-19 patients. Please note that these results were published in [117].

4.3 Evaluation of automated immunoassays

4.3.1 Performance assessment of assay sensitivity and specificity

The performance of the five selected automated analyzers was assessed for the detection of antibodies from samples collected from COVID-19 patients (n=110). The overall performance of each assay is shown in Figure 15 and Table 6. The highest sensitivity was demonstrated by VITROS® at 99.0%, followed by CL-900i® at 90.1%, and VIDAS®3 at 88.2%, then LIAISON®XL at 85.6%, and Architect placing at last with the lowest sensitivity at 80.0%. The specificity of each automated immunoassay was assessed using pre-pandemic sera samples seropositive for various respiratory and non-respiratory viruses. Figure 15 and Table 6 show that three immunoassays demonstrated 100% specificity, including LIAISON®XL, Abbott architect, and VITROS®. VIDAS®3 also showed a very good overall specificity, cross-reacting with only two samples (one seropositive for non-CoV respiratory viruses and one seropositive for ANAs). CL-900i®, however, demonstrated the lowest specificity at 95.3%, cross-reacting with six seropositive samples for other CoVs.

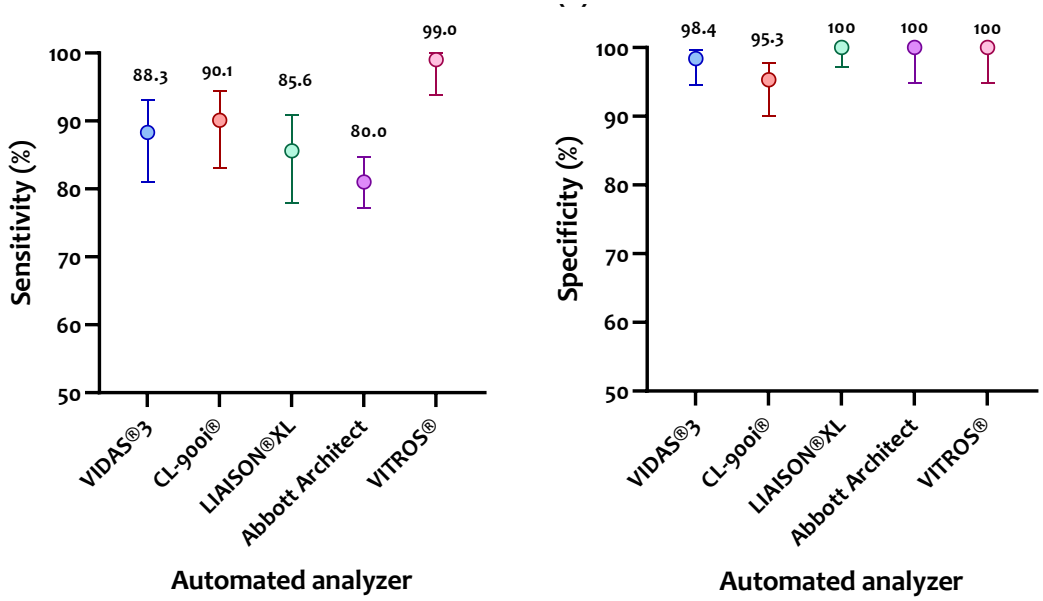

Figure 15. Sensitivity **(A)** and specificity **(B)** of each automated immunoassay in samples collected from RT-PCR confirmed patients (n=110) after 21 days post symptoms onset. Please note that these results were published in [118, 119].

Table 6: Specificity of the four evaluated automated immunoassays according to the negative control subgroups (n=127).

		Specificity (%, 95% confidence interval)				
Subgroup with IgM antibodies against	**No. of samples**	**VIDAS®3**	**CL-900i®**	**LIAISON®XL**	**Abbott Architect**	**VITROS®**
Other coronaviruses (SARS-CoV, MERS-CoV, HCoV-229E, NL63, OC43, and HKU1)	18	18/18; **100** (82.4-100)	12/18; **66.7** (43.8-83.7)	18/18; **100** (82.4-100)	-	-
Non-CoV respiratory viruses (Influenza and RSV)	38	37/38; **97.4** (86.5-99.5)	38/38; **100** (90.8-100)	38/38; **100** (90.8-100)	15/15; **100** (80.8-100)	15/15; **100** (80.8-100)
Non-respiratory viruses (HEV, HGV, HCV, HBV, DENV, WNV, CHIKV, B19, HSV-1, HSV-2, EBV, HHV-6, and HHV-8)	65	65/65; **100** (94.4-100)	65/65; **100** (94.4-100)	65/65; **100** (94.4-100)	51/51; **100** (90.4-100)	51/51; **100** (90.4-100)
Antinuclear antibodies (ANAs)	6	5/6; **83.3** (43.7-97.0)	6/6; **100** (61.0-100)	6/6; **100** (61.0-100)	4/4; **100** (56.0-100)	4/4; **100** (56.0-100)
Overall specificity	127	125/127; **98.4** (94.5-99.6)	121/127; **95.3** (90.1-97.8)	127/127; **100** (97.1-100)	70/70; **100** (94.8–100.0)	70/70; **100** (94.8–100.0)

MERS: Middle East respiratory syndrome coronavirus, SARS-CoV: severe acute respiratory syndrome coronavirus, RSV: respiratory syncytial virus, HSV-1: herpes simplex virus 1, HSV-2 herpes simplex virus 2, HHV-6: human herpesvirus-6, HHV-8: human herpesvirus-8, EBV: Epstein–Barr virus, HBV: hepatitis B virus, HCV: hepatitis C virus, HEV: hepatitis E virus, HGV: hepatitis G virus, B19: parvovirus B19, WNV: West Nile virus. Please note that these results were published in [118, 119].

4.3.2 Performance assessment of automated immunoassays using sVNT as reference test

The performance assessment of five automated analyzers was assessed in comparison with GenScript sVNT to assess how they correlate with neutralizing activity. As shown in Table 7, all immunoassays showed sensitivities above 90%, except Architect standing at 81.0% (95% CI: 77.2–84.7) overall sensitivity. VITROS® demonstrated the highest estimated sensitivity at 99.0% (95% CI: 93.8–100.0), followed by CL-900i at 96.1% (95% CI: 90.4–98.5%), VIDAS®3 at 95.1% (95% CI: 89.1–97.9%), and then LIAISON®XL at 92.2% (95% CI: 85.4–96.0%).

Concordance assessment for each immunoassay and sVNT showed an overall agreement ranging between 88.6% (83.9–93.3) for Architect and 99.3% (97.9–100.0) for VITROS®. Cohen's Kappa statistic also denoted good to excellent agreement ranging between 0.63 (0.52-0.74) for LIAISON®XL and 0.98 (0.96–1.0) for VITROS®.

Table 7. Performance and concordance assessment between each automated immunoassay and the sVNT. Please note that these results were published in [118, 119].

Automated assay	**VIDAS®3**	**CL-900i®**	**LIAISON®XL**	**Abbott Architect**	**VITROS®**
Sensitivity % (95% CI)	95.1 (89.1–97.9)	96.1 (90.4–98.5%)	92.2 (85.4–96.0)	81.0 (77.2–84.7)	99.0 (93.8–100.0)
Specificity % (95% CI)	98.4 (94.5-99.6)	95.3 (90.1-97.8)	100 (97.1-100)	100.0 (94.8–100.0)	100.0 (94.8–100.0)
Overall agreement % (95% CI)	95.5 (89.9-98.1)	95.5 (89.9-98.1)	92.8 (86.4-96.3)	88.6 (83.9–93.3)	99.3 (97.9–100.0)
Cohen's kappa coefficient κ (95% CI)	0.74 (0.65-0.83)	0.93 (0.89–0.97)	0.63 (0.52-0.74)	0.77 (0.71–0.84)	0.98 (0.96–1.0)
ROC curves optimized cut-off index	>0.48	>7.86	>4.78	>0.87	>0.91
Sensitivity using optimized cut-off indices % (95% CI)	93.7 (88.5-97.6)	98.1 (93.3–99.7)	92.8 (86.4-96.3)	87.6 (79.9– 92.6)	99.0 (94.7–99.9)
Specificity using optimized cut-off indices % (95% CI)	98.4 (94.5-99.6)	100.0 (94.8–100.0)	100.0 (94.8–100.0)	100.0 (94.8–100.0)	100.0 (90.4–100.0)

4.3.3 Receiver operating characteristics (ROC) curve analysis

ROC curve analysis was performed and summarized in Table 7 and Figure 16. As shown in Figure 16, ROC curve analyses indicated that all five assays had an AUC above 0.96, indicating an excellent performance (VIDAS®3: 0.97, CL-900i®: 0.97, LIAISON®XL: 0.96, Architect: 0.9966, VITROS®: 0.9997, $p < 0.0001$). Based on the ROC curves and calculated Youden's index, optimized thresholds (cutoff indices) for detecting anti-SARS-CoV-2 Abs that correlate with the sVNT were obtained. The derived cut-off indices were >0.48 for VIDAS®3, >7.86 for CL-900i®, >4.78 for LIAISON®XL, >0.87 for Architect, and >0.91 VITROS®, respectively, compared to the manufacturer's suggested cut-offs which were ≥1.0, ≥10.0, ≥15.0, ≥1.4, and ≥1.0, respectively. By applying these new cutoff values, CL-900i® and Architect showed an improved overall sensitivity (98.1% and 87.6%, respectively). Whereas the sensitivity remained the same for LIAISON®XL and VITROS® (92.8% and 99.0%, respectively), it slightly decreased to 93.7% for VIDAS®3 assay. The new cutoff values did not affect the specificity of all assays, except for CL-900i® , which showed an increase reaching 100%.

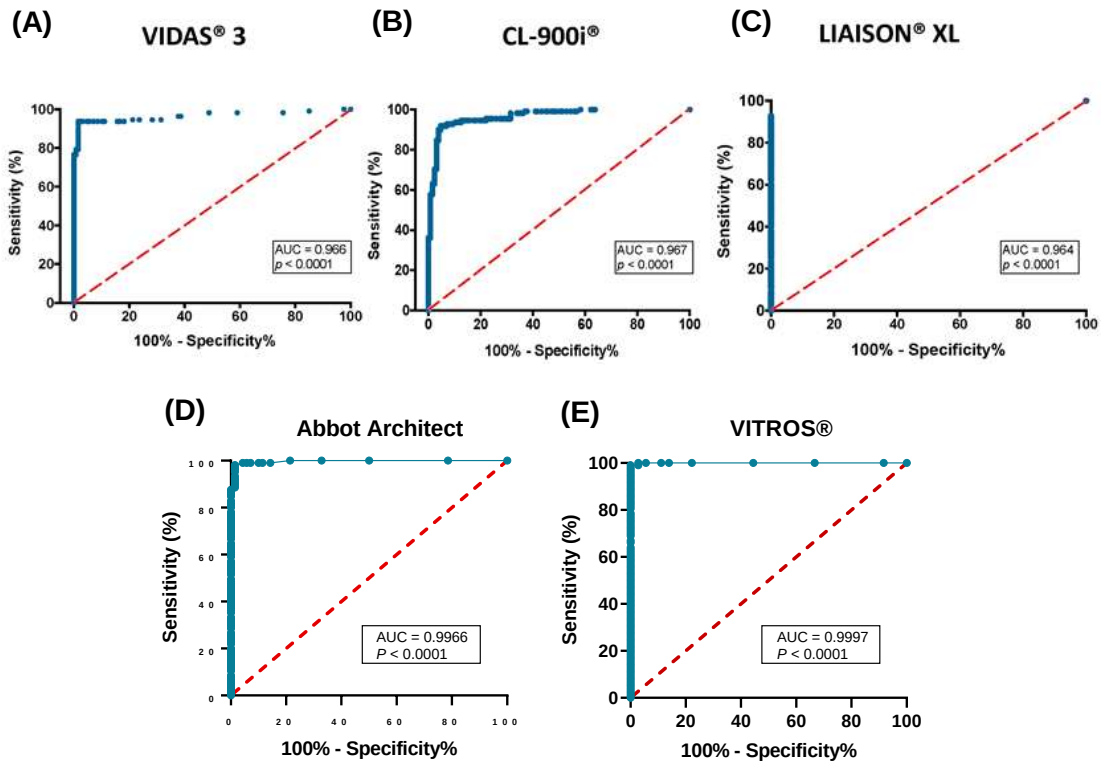

Figure 16. Empirical Receiver Operating Characteristic (ROC) curve analysis for each automated immunoassay: VIDAS®3 **(A)**, CL-900i® **(B)**, LIAISON®XL **(C)**, Architect **(D)**, and VITROS® **(E)**, to estimate the optimal threshold levels for predicting the presence of NAbs against SARS-CoV-2. The sensitivity and specificity values correspond to the plotted points in the graphs which were used to calculate the area under the curve (AUC) and *p*-value for each curve plot. Based on the area under the ROC curve, the Youden Index cutoff values that maximize the sum of sensitivity and specificity were determined. An AUC of 0.9–1.0 is considered excellent, 0.8–0.9 very good, 0.7–0.8 good, 0.6–0.7 sufficient, 0.5–0.6 bad, and less than 0.5 considered not useful. The significance level was set at 0.05. Please note that these results were published in [118, 119].

4.3.4 Correlation analysis between automated immunoassays and sVNT

Correlation and linear regression analysis between the values obtained from each automated immunoassay and neutralizing activity (percent inhibition) obtained by sVNT is shown in Figure 17. Spearman's correlation coefficient (ρ) showed a statistically significant positive correlation for all assays with neutralizing activity ($p < 0.001$). The strength of correlation ranged from weak to strong where the strongest correlation was shown by three assays including VIDAS®3 ($\rho = 0.729$, Figure 17A), VITROS® ($\rho = 0.718$, Figure 17E), and CL-900i® ($\rho = 0.712$, Fig. 17B). Architect immunoassay, which targets SARS-CoV-2 N protein demonstrated a moderate correlation with sVNT ($\rho = 0.618$, Figure 17D), whereas LIAISON®XL had the weakest correlation ($\rho = 0.415$, Figure 17C). Linear regression analysis showed that all constructed models could statistically significantly predict the dependent variable (% inhibition) based on the cutoff index (COI) generated by each immunoassay with a predication precision ranging between 13.9–21.9% (standard error of estimate, SEE). The best regression model fitting the data was obtained by VIDAS®3 ($r^2 = 905$, SEE = 18.1%).

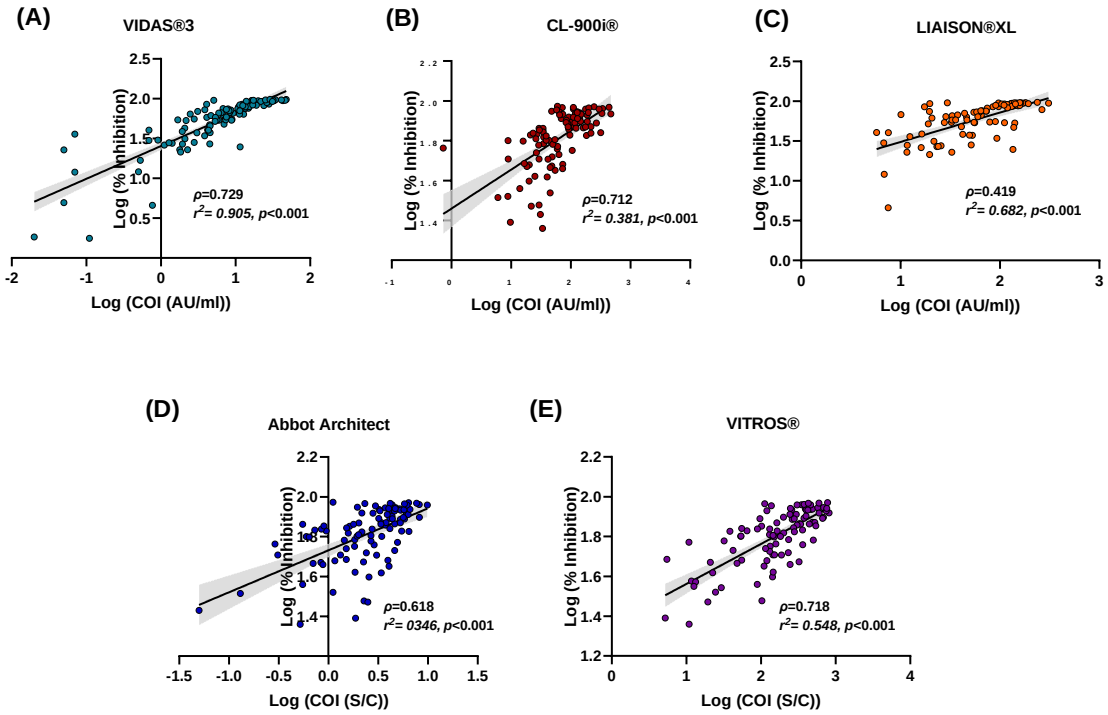

Figure 17. Correlation and linear regression analysis between log-transformed values obtained from each automated immunoassay and the log-transformed percent inhibition (%) results**.** Spearman's correlation coefficient (ρ), r^2, and *p*-value are shown for each model. Correlation coefficients (ρ) can be interpreted as follows: <0.3 is negligible, 0.3–0.5 is weak, 0.5–0.7 is moderate, 0.7–0.9 is strong, and >0.9 is very strong. Please note that these results were published in [118, 119].

4.4 Evaluation of surrogate virus neutralization immunoassays (sVNT)

The performance assessment of two sVNTs, developed by GenScript and Mindray, in comparison with pVNT reference test is summarized in Figures 18-20.

4.4.1 Performance assessment of sVNT assays

To validate the performance of both SARS-CoV-2 sVNT assays, samples collected from previously SARS-CoV-2 infected and vaccinated individuals were assessed. Figure 18 shows the dot plot distribution of values obtained from each assay per tested sample group. All neutralization assays demonstrated a clear separation between

known positive and known negative samples resulting in 100% specificity with 100% sensitivity for GenScript and Dynamiker sVNT and 100% specificity with 99.5% sensitivity for Mindray NTAb sVNT.

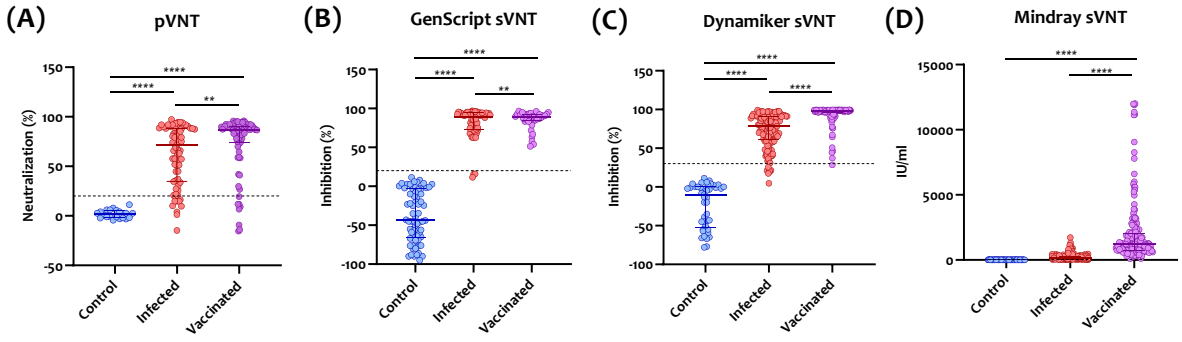

Figure 18. Dot plot of neutralizing antibody readings obtained from **(A)** Pseudovirus neutralization test (pVNT), **(B)** SARS-CoV-2 sVNT from GenScript, **(C)** SARS-CoV-2 sVNT from Dynamiker, and **(D)** SARS-CoV-2 sVNT from Mindray CL900i, using samples collected from healthy controls, previously SARS-CoV-2 infected patients, and vaccinated individuals. Individual points obtained, median values and interquartile ranges (IQR) are shown. The dotted lines represent the cutoff at 20% inhibition for pVNT, 30% for GenScript's and Dynamiker's sVNT and at 33.1 international unit per ml (IU/ml) for Mindray's sVNT. P values were calculated using one-way analysis of variance (ANOVA) test. *p< 0.05, ***p< 0.001, **** p<0.0001.

4.4.2 Correlation analysis

Correlation and linear regression analysis between pVNT and each sVNT assay was performed. A total of 54 sera samples, collected from previously infected COVID-19 patients and vaccinated individuals, were chosen to assess the correlation between each sVNT with pVNT . As shown in Figure 19, GenScript's and Mindray's sVNTs had a strong overall correlation with the pVNT, whereas Dynamiker's sVNT showed

a slightly lower correlation.

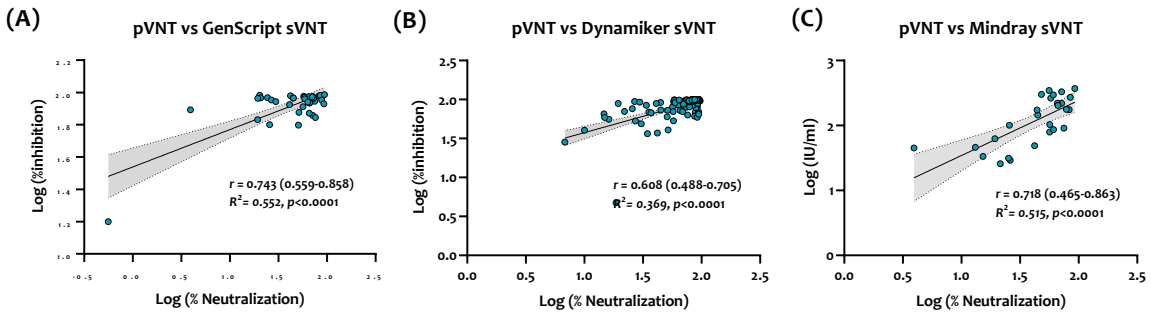

Figure 19. Correlation and linear regression analysis for convalescence sera collected from previously infected COVID-19 patients and vaccinated individuals (n= 41) between **(A)** pVNT and GenScript's sVNT, and between **(B)** pVNT and Dynamiker's sVNT, and (C) pVNT and Mindray CL900i sVNT. Correlation and linear regression analyses were performed in GraphPad Prism using Pearson's correlation coefficients (r) and R^2. Statistical significance was calculated using the two-tailed test. Presented data are the log of neutralization (%) by pVNT and log of inhibition results (%) by sVNT assays or IU/ml. The dashed lines indicate the 95% confidence intervals of the linear regression plots.

4.4.3 ROC curve analysis

As shown in Figure 20, ROC curve analyses demonstrated excellent performance for all three sVNT assays in samples collected from SARS-CoV-2 infected patients, and COVID-19 vaccinated individuals with an AUC ranging between 0.99-1.0 (p<0.0001). Based on the ROC curves and calculated Youden's index, optimized thresholds (cut-off indices) for detecting NAbs by each assay were obtained. The derived cut-off indices for GenScript sVNT were >17.11% inhibition in SARS-CoV-2 infected cohort and >31.37% in the vaccinated cohort compared to the manufacturer's suggested cut-off (≥30% inhibition). Furthermore, derived cut-off indices for Mindray sVNT were >51.32 international unit per ml (IU/ml) in SARS-

CoV-2 infected cohort and >24.18 IU/ml in the vaccinated cohort compared to the manufacturer's suggested cut-off (≥33.1 IU/ml). As for Dynamiker sVNT, derived cut-off values were >14.39 % in SARS-CoV-2 infected cohort and >19.85% in the vaccinated cohort compared to the manufacturer's suggested cut-off (≥30% inhibition). Applying these new cut-off values did not seem to affect the already established specificity of all assays. However, the sensitivity was slightly increased for GenScript and Dynamiker to 100% and 99.2%, respectively, indicating that the cut-off can be adjusted based on the tested cohort without significantly affecting the assay's performance.

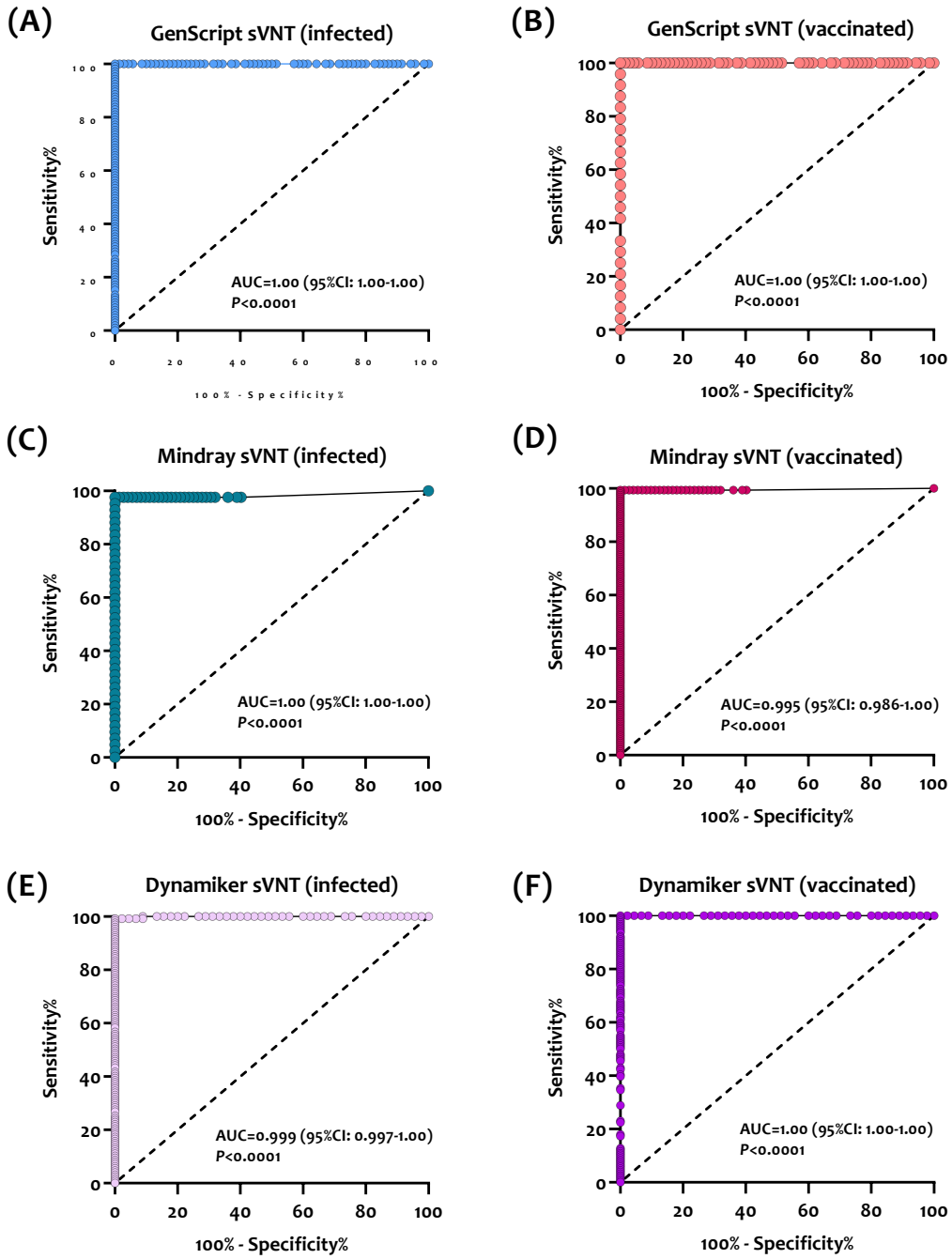

Figure 20. Empirical receiving operating characteristic (ROC) curve analysis for estimating optimal thresholds for sVNT assays targeting nAbs against SARS-CoV-2. **(A)** GenScript sVNT ROC curve in SARS-CoV-2 infected patients (n=105). **(B)** GenScript sVNT ROC curve in COVID-19 vaccinated individuals (n=24). **(C)** Mindray sVNT ROC curve in SARS-CoV-2 infected patients (n=52). **(D)** Mindray sVNT ROC curve in COVID-19 vaccinated individuals (n=155). **(E)** Dynamiker sVNT ROC curve

in SARS-CoV-2 infected patients (n=127). **(F)** Dynamiker sVNT ROC curve in COVID-19 vaccinated individuals (n=156). The sensitivity and specificity values correspond to the plotted points which were used to estimate the area under the curve (AUC) and *p*-value for each curve.

4.5 ADCC activity

ADCC activity against SARS-CoV-2 S and N proteins was analyzed using samples collected from previously infected and vaccinated individuals. A total of 90 samples collected from symptomatic (n=42) and asymptomatic (n=48) COVID-19 patients were included in addition to 77 samples from vaccinated individuals with BNT162b- (n= 40) or mRNA-1273 (n=37) COVID-19 vaccines.

4.5.1 SARS-CoV-2-specific ADCC activity following infection and vaccination

Among all previously infected individuals, 81 out of 90 (90.0%) had ADCC activity against SARS-CoV-2 S protein above 2-fold induction compared to only 42 out of 77 (54.5%) vaccinated individuals (Figure 21A). On the other hand, 49 out of 73 (67.1%) infected individuals had ADCC activity against SARS-CoV-2 N protein compared to 15 out of 65 (23.1%) vaccinated individuals (Figure 21B). Symptomatic COVID-19 patients showed higher ADCC activity against SARS-CoV-2 S protein, ranging from 0.9 to 9.5-fold induction, compared to asymptomatic (0.8-5.3-fold induction) and vaccinated individuals with either Pfizer (0.3-5.2-fold induction) or Moderna vaccines (0.1-7.3- fold induction) as shown in Figure 21C. Moreover, ADCC activity against SARS-CoV-2 N protein was significantly higher in symptomatic individuals, ranging from 1.1 to 19.1-fold induction, compared to Pfizer-vaccinated (0.7-9.2-fold induction) and Moderna-vaccinated (0.4-5.5-fold induction) Figure 21D.

Differences in ADCC activity in relation to age and gender were evaluated, which showed a significant difference in overall activity against SARS-CoV-2 S and N proteins between males and females (p=0.0015 and p=0.0172, respectively) as shown in Figure 22. However, when assessing ADCC among previously infected and vaccinated individuals, no significant difference was observed between the genders. Moreover, as shown in Figure 23, a significant difference in ADCC activity against S protein was revealed between individuals within the age group 19-30 years and 50-60 years (p=0.0015) as well as infected individuals within the age group 31-40 and 51-60 years (p=0.0365).

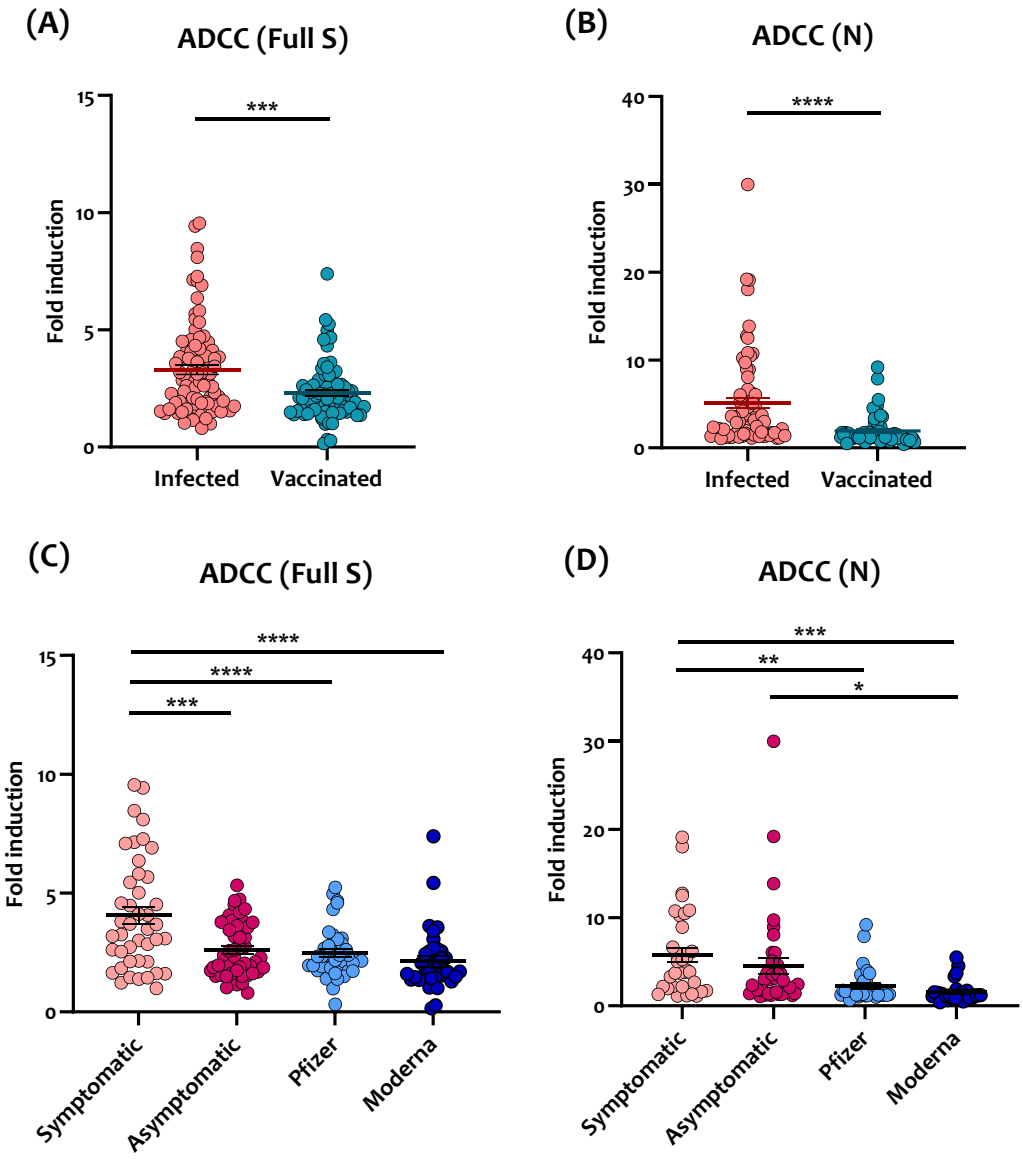

Figure 21. ADCC activity against SARS-CoV-2 full spike (S) protein **(A)** and nucleocapsid (N) protein **(B)** in infected (n=90) vs. vaccinated (n=77) individuals. ADCC activity against full S **(C)** and N **(D)** proteins in symptomatic (n=42), asymptomatic (n=48), BNT162b2- (n= 40) and mRNA-1273-vaccinated (n=37) individuals. P values were calculated from unpaired two-tailed Student's t-tests and one-way analysis of variance (ANOVA) test.

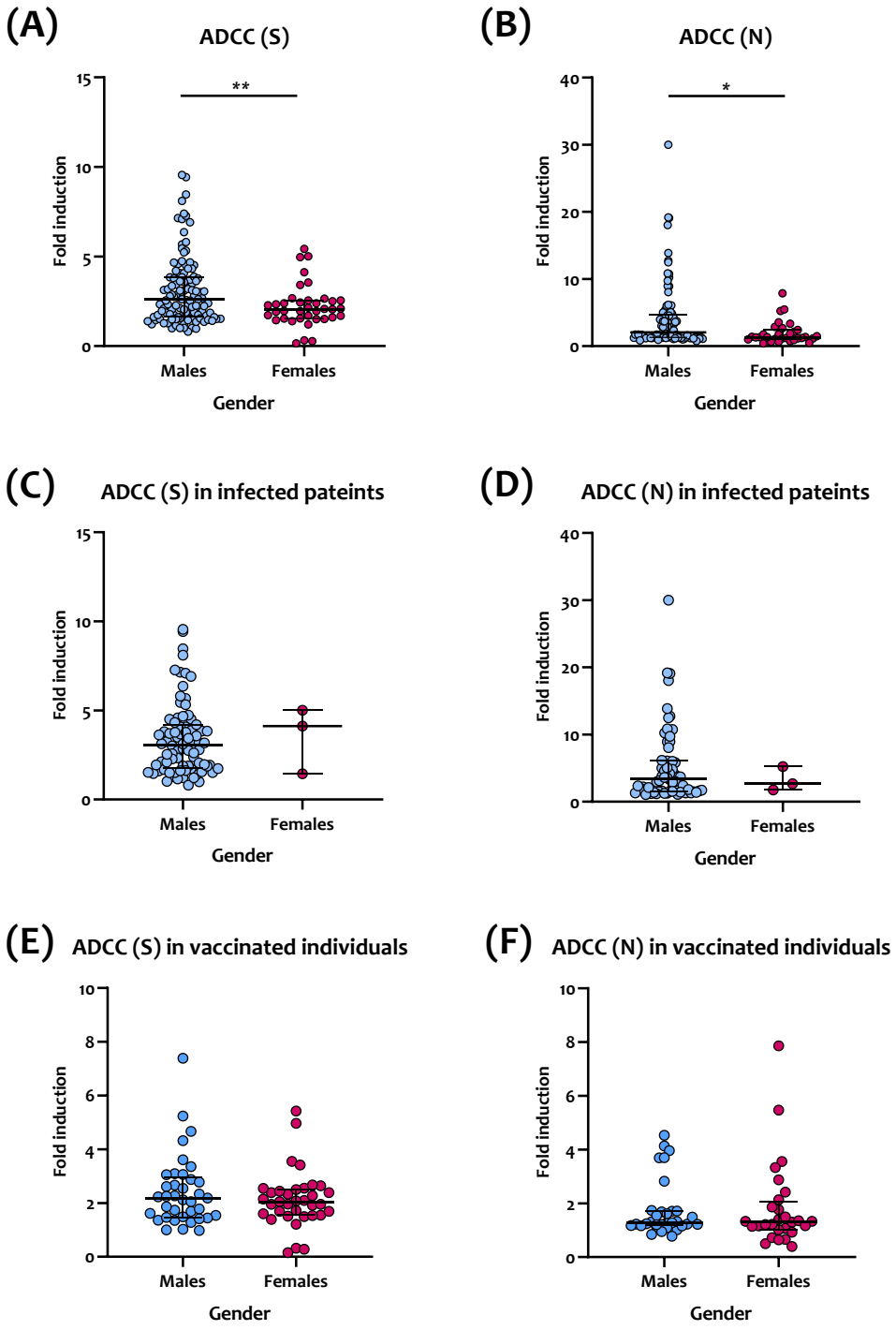

Figure 22. Antibody-dependent cellular cytotoxicity (ADCC) activity in previously infected (n=83) and vaccinated (n=72) individuals stratified by gender (117 males and 38 females). ADCC against S protein **(A)** and N protein **(B)** in total participants (n=155). ADCC against S and N proteins is also shown for previously infected **(C, D)**

and vaccinated individuals **(E, F)**. Unpaired t-test was used to compare between the two groups.

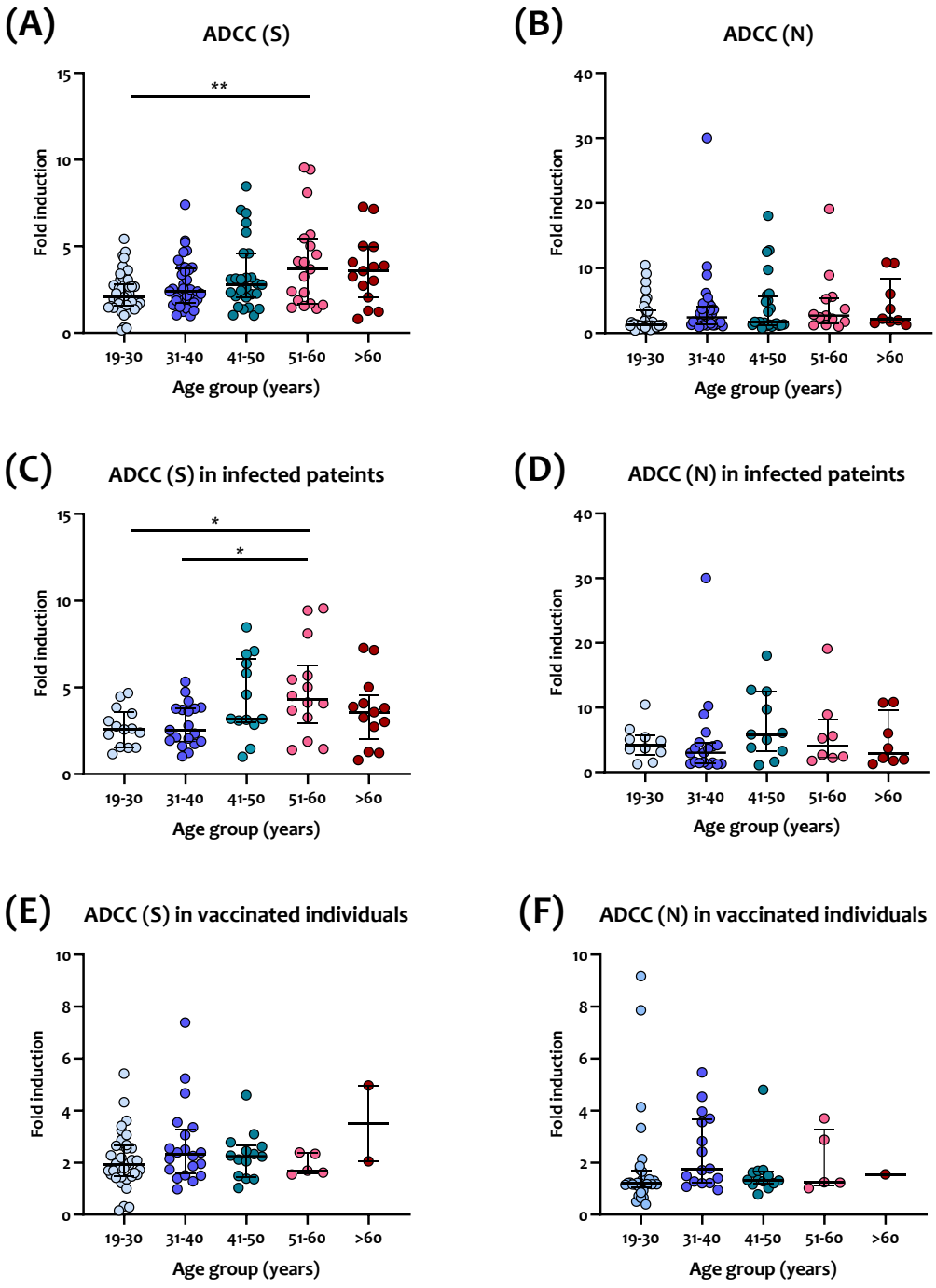

Figure 23. ADCC activity in previously infected (n=63) and vaccinated (n=77) individuals stratified by age groups. ADCC against S protein **(A)** and N protein **(B)** in total participants (n=140). ADCC against S and N proteins is also shown for previously infected **(C, D)** and vaccinated individuals **(E, F).** The multiple comparisons among the groups were made using one-way analysis of variance (Kruskal–Wallis test) followed by Bonferroni post hoc correction.

4.5.2 ADCC activity over time

When all sampling time-points (for both infected and vaccinated) were combined for analysis, ADCC activity against both S and N proteins was detectable within the first 10 days of sampling (post symptoms onset or second dose administration). As shown in Figure 24A, ADCC activity reached its peak within 11-20 days against S protein (median= 3.30, interquartile range (IQR)= 2.17-5.32) and within 21-30 days against N protein (median= 4.58, IQR= 1.20-9.64), then it remained at comparable levels until the last observation at two months (Figure 24B). When assessing ADCC activity in infected vs. vaccinated individuals, no significant difference was observed across the different time-points where ADCC was maintained at comparable levels until the last observation at one month post infection (Figure 24 C, D) and two months post second dose of vaccine administration (Figure 24E and 24 F).

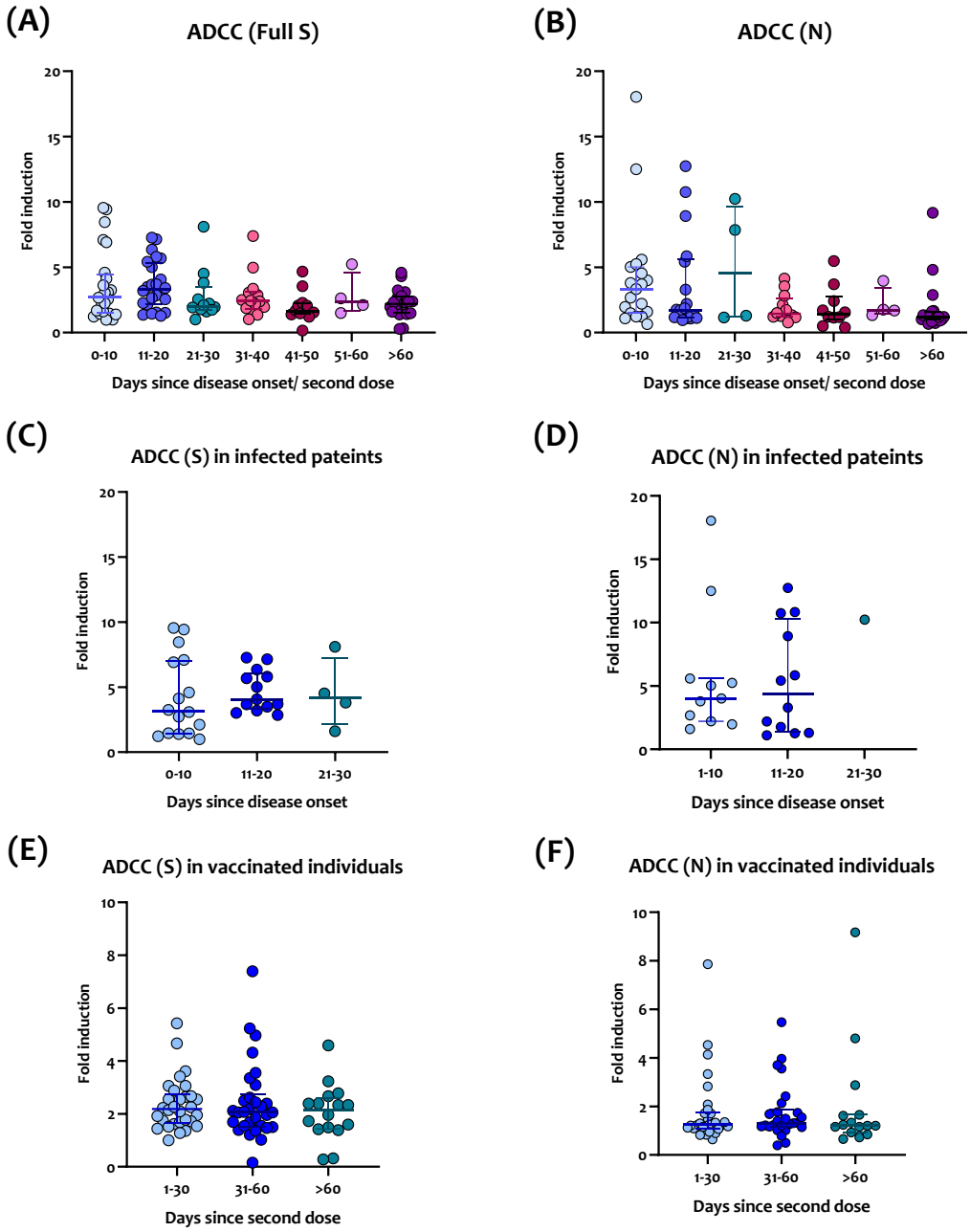

Figure 24. ADCCactivity in previously infected (n=33) and vaccinated (n=76) individuals over time. ADCC against S protein **(A)** and N protein **(B)** in total participants (n=110). ADCC against S and N proteins is also shown for previously infected **(C, D)** and vaccinated individuals **(E, F).** The multiple comparisons among the groups were made using one-way analysis of variance (Kruskal–Wallis test) followed by Bonferroni post hoc correction.

4.5.3 Correlation between ADCC with binding antibodies and NAbs

Correlation and linear regression analysis were performed to correlate ADCC activity with binding and NAbs targeting cognate SARS-CoV-2 proteins (Figure 25). Correlation between ADCC against the S and N proteins and IgG binding antibodies against both proteins showed good correlation (r=0.613 and r=637, respectively) as shown in Figures 25A and 25B. Further, ADCC activity against the S protein and IgG antibodies targeting S protein and RBD also showed a good correlation with r=0.608 and r=0.668, respectively (Figure 25 C, D). However, a weak correlation between ADCC against the S protein and total binding antibodies targeting the RBD was observed (r= 0.358, Figure 25E).

ADCC activity was also correlated with NAbs against SARS-CoV-2 S protein, and RBD detected by pVNT and sVNT, respectively. As shown in Figure 26 below, similar results were obtained for both assays showing a moderate-strong correlation between ADCC and NAbs (r=0.640 for pVNT, and r=0.760 for sVNT)

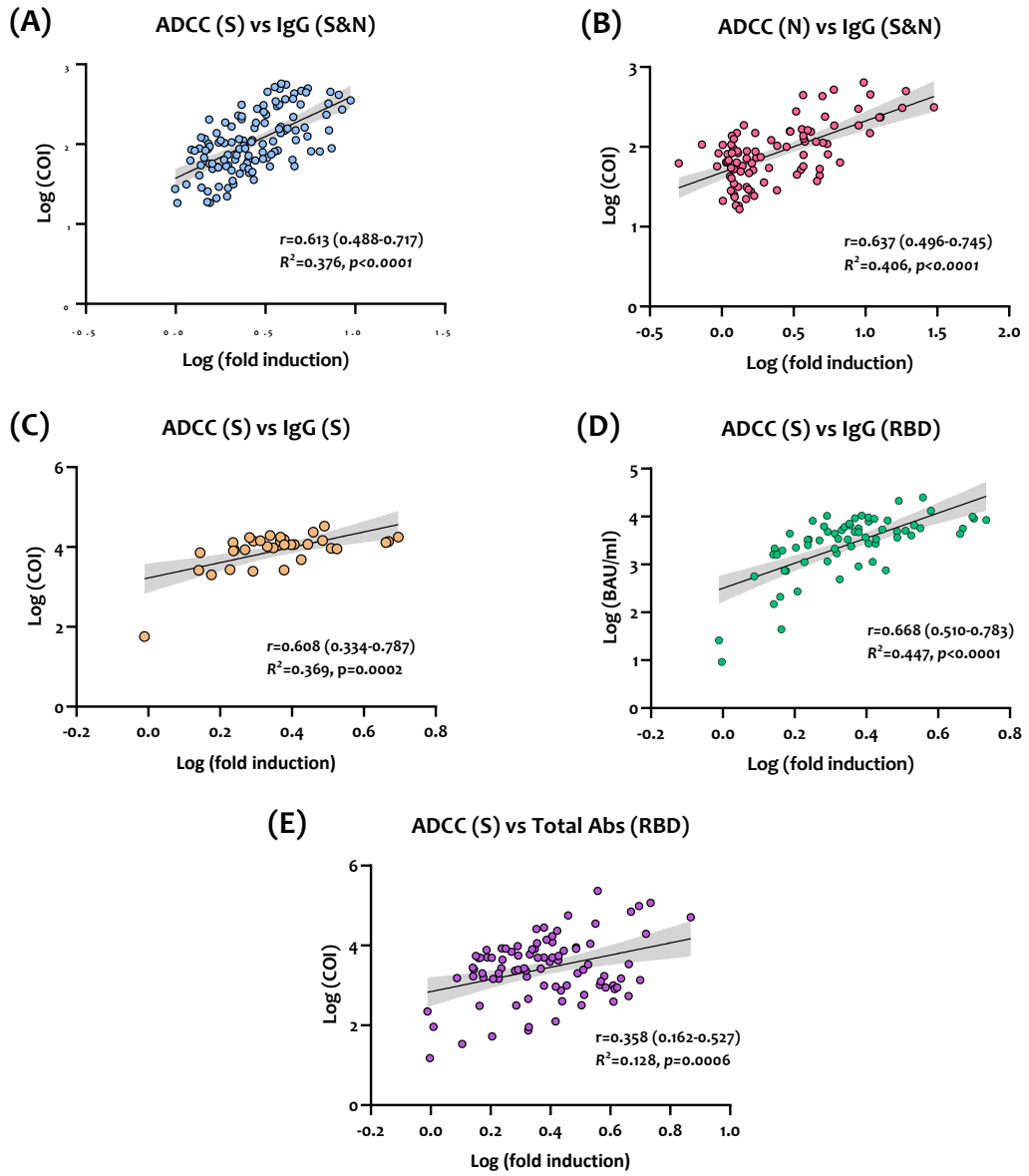

Figure 25. Correlation and linear regression analysis between ADCC and anti-SARS-CoV-2 binding antibodies for convalescence sera collected from previously infected COVID-19 patients and vaccinated individuals (n= 127). Log transformed values were plotted for **(A)** ADCC fold induction by S protein with binding IgG antibodies against SARS-Cov-2 S and N protein, **(B)** ADCC against N protein with binding IgG antibodies against S and N protein, **(C)** ADCC against S protein with binding IgG antibodies against S protein, **(D)** ADCC against S protein with binding IgG antibodies against RBD, **(E)** ADCC against S protein with total binding antibodies against SARS-CoV-2

RBD. Pearson correlation coefficient (r) with 95% confidence interval (95% CI), R^2, and *p*-value are shown for each model. Correlation coefficients (r) can be interpreted as follows: <0.3 is negligible, 0.3–0.5 is weak, 0.5–0.7 is moderate, 0.7–0.9 is strong and >0.9 is very strong.

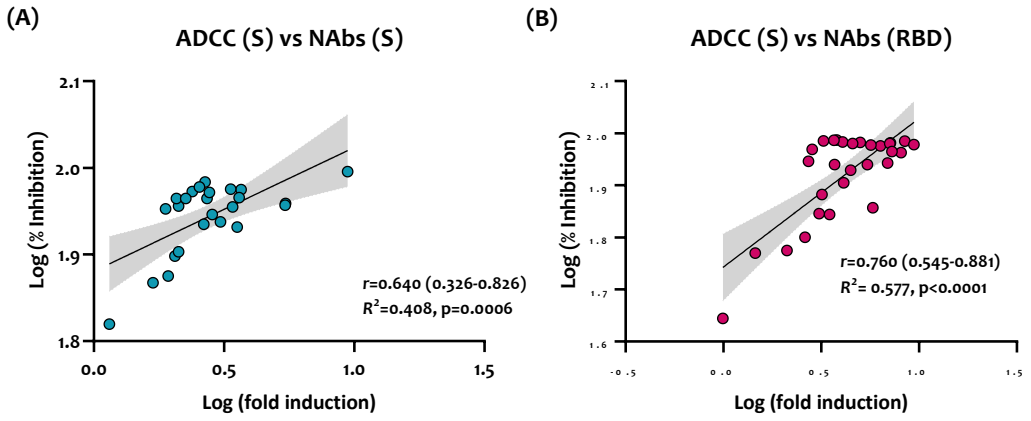

Figure 26. Correlation and linear regression analysis between ADCC and anti-SARS-CoV-2 NAbs for convalescence sera was collected from previously infected COVID-19 and vaccinated individuals**.** Log transformed values were plotted for **(A)** ADCC fold induction by S protein with NAbs detected by pVNT targeting SARS-CoV-2 S protein, n=29, **(B)** ADCC fold induction by S protein with NAbs detected by sVNT targeting SARS-CoV-2 RBD, n=25. Pearson correlation coefficient (r) with 95% confidence interval (95% CI), R^2, and *p*-value are shown for each model.

CHAPTER 5: DISCUSSION

Since the beginning of the COVID-19 pandemic, a consensus has emerged that serological tests provide an essential tool in the pandemic response, but inadequate data on the performance characteristics of these tests in some early surveys and gaps in immunological knowledge have hindered agreement on the choice of reliable immunoassays [120]. As described in the Interim Guidelines for COVID-19 Antibody Testing published by the CDC [121], the currently available serologic assays measure binding antibodies targeting SARS-CoV-2 antigens and functional antibodies (or NAbs), which neutralize the virus via conventional neutralization assays (live or pseudovirus) or surrogate virus neutralization tests (sVNT). The most common antigenic targets employed by these assays include the N protein, S protein, and RBD. In this project, the humoral immune responses against SARS-CoV-2 were characterized in previously infected, and COVID-19 vaccinated individuals to assess and identify the correlates of protective immunity. For this purpose, we first evaluated the performance of different commercial manual and automated immunoassays to detect anti-SARS-CoV-2 binding antibodies and NAbs. A total of nine manual IgM and IgG ELISA kits, five automated immunoassays, and two sVNT assays were assessed using samples collected from previously SARS-CoV-2-infected and mRNA-vaccinated individuals. Results showed heterogenous assay performance for IgM ELISA kits, whereas IgG ELISA kits targeting SARS-CoV-2 S protein showed a good-excellent overall performance. IgM antibodies are naturally known to have a lower affinity for viral antigens than IgG, and hence, serological tests targeting IgM are at higher risk of producing inaccurate results. Previous studies also showed variable performances for IgM serological tests [122, 123]. Consistent with the literature, our data showed that IgM and IgG tend to rise around the same time

following SARS-CoV-2 infection [124, 125]. Further, seropositive rates for IgG increased with time, peaking in samples collected after 20 post-symptoms onset or positive RT-PCR tests. Higher seropositive rates were observed among symptomatic COVID-19 patients than the asymptomatic counterparts, suggesting good to excellent sensitivity in this patient cohort.

Moreover, automated immunoassays targeting anti-SARS-CoV-2 IgG antibodies demonstrated similar results to manual ELISA kits, where assays targeting the S protein and RBD showed the best performance in terms of sensitivity, specificity, and agreement. We also aimed to identify the extent to which these automated serology assays correlate with neutralization, and therefore, correlation analysis in comparison with a reference neutralization assay was performed. Expectedly, automated assays targeting SARS-CoV-2 s protein, particularly RBD, showed the best correlation with neutralizing activity, suggesting that they could serve as reliable and high-throughput assays for predicting the presence of protective NAbs.

Despite the good performance and correlation with neutralizing activity seen by the assessed commercial serological tests, direct detection of NAbs is still of crucial importance. Hence, the extent to which positive results by serology reflect a protective immune response is still insufficient for assessing protective immunity. Fortunately, since the COVID-19 pandemic, a handful of commercial immunoassays have been developed to serve as surrogate assays for conventional virus neutralization assays [107]. Of which, two assays were selected and evaluated in this project, including GenScript sVNT and Mindray NTAb sVNT. Both assays detect NAbs targeting SARS-CoV-2 RBD and have shown excellent performance and correlation with pVNT in samples collected from previously infected SARS-CoV-2 patients and vaccinated individuals. In addition, the performance of GenScript sVNT was

previously validated in a study conducted on two COVID-19 patients' cohorts in two different countries and showed that the assay is as specific as, and even more sensitive than, cVNT and pVNT [107].

Although it is known that not all NAbs are necessarily RBD-binding, as shown by previous studies on SARS-CoV, which indicated that NAbs targeting other regions of S1 and S2 proteins are also generated [65]. However, studies have shown that the RBD is the immunodominant target for NAbs suggesting that non-RBD-targeting antibodies measured by cVNT and pVNT are unlikely to play a major role in neutralizing SARS-CoV-2, consistent with previous findings [126-128]. Therefore, it can be said that RBD-based sVNTs could serve as robust platforms for reliable and high-throughput testing for RBD-targeting NAbs. Another key advantage offered by these sVNTs over most ELISA or point-of-care serological tests is their ability to detect total NAbs in an isotype-independent manner, hence, increasing the test sensitivity.

While NAbs play a critical role in interfering with a viral infection, other non-NAbs immune mechanisms mediated by Fc receptors can also contribute to preventing SARS-CoV-2 infection and limiting COVID-19 severity. Still, the direct correlation with protection is not clearly defined yet. Fc-dependent ADCC effector functions were previously shown to play a role in the protection and pathogenesis of various infectious pathogens [129-132]. Several innate effector cells are capable of inducing the ADCC effect in vitro; however, NK cells have been proposed to be the major contributors to ADCC in vivo [133]. ADCC-inducing antibodies were previously identified as a key correlate of protection against several viral infections, including Dengue fever, Ebola, and human immunodeficiency virus (HIV) [15, 134, 135]. Nevertheless, the role of ADCC in influenza is still debatable, with some studies

suggesting a protective capacity of ADCC-inducing antibodies [18], whereas others show no role or exaggeration of the immune response by ADCC [136-138]. In terms of COVID-19, the exact role of ADCC activity has not been fully delineated yet, with only a few studies investigating Fc-mediated effector functions.

While vaccines are currently regarded as the primary preventative measure against COVID-19, concerns about their effectiveness against SARS-CoV-2 VOCs are rising due to a large number of reported breakthrough infections among people who received 2-3 jabs. Here, ADCC activity was assessed to identify other correlates of protection against SARS-CoV-2. For this purpose, samples collected from previously infected and vaccinated individuals were analyzed. We found significantly higher ADCC against SARS-CoV-2 S in infected than in vaccinated individuals (mean fold induction =3.3 in infected vs. 2.3 in vaccinated). Interestingly, significant ADCC activity against the N protein was also observed previously infected vaccinated individuals (mean fold induction =5.1 in infected vs. 1.9 in vaccinated), suggesting possible prior exposure and infection with SARS-CoV-2 among the vaccinated cohort, although not documented.

Moreover, our study revealed significantly elevated ADCC activity against both SARS-CoV-2 S and N proteins in symptomatic COVID-19 compared to asymptomatic and vaccinated cases, which raises questions about whether ADCC response may contribute to pathology. It has been previously reported that during viral infection, elevated ADCC responses could induce inflammation [139], suggesting a potential role for ADCC in COVID-19 pathogenesis. Contrarily, elevated ADCC response in severe patients could be a result of prolonged SARS-CoV-2 infection with high viral load leading to persistent antigen exposure in these patients. However, it is possible that the timely induction of ADCC might play a role in determining the

clinical outcome. Previous studies reported a correlation between delayed NAbs production and severe COVID-19 and mortality [111]. Hence, a similar mechanism might be involved in ADCC by which the timing of antibody production plays a critical role in determining the clinical outcome. That being said, patients who develop delayed ADCC response might succumb to more severe disease. A possible explanation is that during the early stages of the disease, cells mediating ADCC might become functionally compromised and thus deprives the host of eliciting ADCC responses. Regardless, further studies with a larger sample size are warranted to test this hypothesis.

We also found that peak levels of ADCC were reached around 11-20 days for S protein which was earlier than the reported peak time of NAbs, about three weeks after disease development [59, 111]. Further, ADCC activity remained relatively stable until the last sampling point at two months post-infection or second dose administration. A recent study assessing ADCC against SARS-CoV-2 S protein also showed relatively stable ADCC levels until one-year post-infection [59], indicating the possible application of ADCC as a marker of infection than NAbs, which extends the window beyond that inferred from neutralizing activity. Still, this still needs to be confirmed by testing more samples collected at more time-points post-infection and vaccination. Additionally, it has been reported that asymptomatic individuals generate robust antibody responses against SARS-CoV-2 S and N proteins [140]. Our findings also showed high ADCC activity elicited in asymptomatic individuals, comparable to the activity induced by vaccinated individuals. Of note, mRNA vaccines did not seem to induce significant ADCC responses compared to natural infection, although these vaccines were shown to induce robust NAb titers [76, 84, 141]. Furthermore, increasing evidence is showing that the newly emerged SARS-CoV-2 variants resist

neutralizing activity induced against the wild-type SARS-CoV-2 [142]. Non-RBD binding antibodies induced after a single dose of BNT162b2 vaccine were reported to lack the ability to mediate neutralizing activity but are capable of mediating ADCC [143]. Another study also showed that anti-RBD antibodies correlate with strong neutralizing activity with weak ADCC activity, whereas antibodies elicited by S2 protein correlate with weaker neutralizing activity and stronger ADCC activity [59]. This suggests that non-NAbs targeting SARS-CoV-2 might have a potential ADCC activity. Therefore, in the context of emerging neutralization-resistant VOCs, Fc-dependent ADCC effector functions might help identify antigenic targets with extra-neutralization activity since we have shown that multiple antigens can mediate ADCC responses to SARS-CoV-2 with high activity levels.

CHAPTER 6: CONCLUSION

Since appropriate use and interpretation of serological tests for assessments of SARS-CoV-2 exposure and potential immunity require accurate data on assay performance, we assessed the performance of several commercial immunoassays to identify reliable assays for the detection of anti-SARS-CoV-2 humoral responses. The extent to which these conventional serology assays correlate with neutralization was shown to depend on the antigen targeted by these assays and on the time of sample collection post disease onset. Further, FcγR-binding ADCC response was identified as a major trait of symptomatic COVID-19 patients and hence may serve as an effective non-NAb response elicited by infection or vaccination against COVID-19. This might help improve our understanding of underlying mechanisms of antibody-mediated immunity, thereby improving the development of vaccine and therapeutic strategies for COVID-19.

CHAPTER 7: LIMITATIONS AND FUTURE DIRECTIONS

Several limitations were faced during this project. First, the lack of a standard test for comparing between our ADCC assay and other ADCC assay formats. Second, instead of using target cells expressing SARS-CoV-2 antigens, 96-well plates were coated with the target protein, and commercially available ADCC bioassay effector cells were used to profile ADCC responses to SARS-CoV-2. In addition, although these effector cells were previously used to assess ADCC activity in several studies [59, 111, 144-146], the use of innate effector cells may provide a better overview of ADCC activity. Also, the conduction of *in vivo* experiments is needed to verify the contribution of ADCC to SARS-CoV-2 infection.

Moreover, ADCC activity was assessed against only two SARS-CoV-2 proteins (S and N). Therefore, investigating ADCC activity against other antigens, including S1, S2, RBD, and N-terminal domain (NTD) could provide more insights into the exact epitopes involved in eliciting ADCC activity. In addition, investigation of the effect of mutations in SARS-CoV-2 proteins that are found in several variants could also help in identifying broadly neutralizing epitopes capable of inducing ADCC responses against myriad variants. Further, it is of paramount importance to assess ADCC cross-reactivity with cognate proteins of other human CoVs to identify if preexisting immunity to such CoVs could induce cross-reactivity or cross-protection against SARS-CoV-2. Therefore, future work might help better assess and understand the exact role of ADCC responses in the context of COVID-19.

REFERENCES

1. Guihot, A., et al., *Cell-Mediated Immune Responses to COVID-19 Infection.* Frontiers in Immunology, 2020. **11**(1662).
2. Güner, R., I. Hasanoğlu, and F. Aktaş, *COVID-19: Prevention and control measures in community.* Turkish journal of medical sciences, 2020. **50**(SI-1): p. 571-577.
3. Fontanet, A. and S. Cauchemez, *COVID-19 herd immunity: where are we?* Nature Reviews Immunology, 2020. **20**(10): p. 583-584.
4. Younes, N., et al., *Challenges in Laboratory Diagnosis of the Novel Coronavirus SARS-CoV-2.* Viruses, 2020. **12**(6).
5. Al-Sadeq, D.W. and G.K. Nasrallah, *The incidence of the novel coronavirus SARS-CoV-2 among asymptomatic patients: A systematic review.* International Journal of Infectious Diseases, 2020. **98**: p. 372-380.
6. Yassine, H.M., et al., *Performance evaluation of five ELISA kits for detecting anti-SARS-COV-2 IgG antibodies.* International Journal of Infectious Diseases, 2021. **102**: p. 181-187.
7. Jeyanathan, M., et al., *Immunological considerations for COVID-19 vaccine strategies.* Nature Reviews Immunology, 2020. **20**(10): p. 615-632.
8. Seow, J., et al., *Longitudinal evaluation and decline of antibody responses in SARS-CoV-2 infection.* medRxiv, 2020: p. 2020.07.09.20148429.
9. Sharma, O., et al., *A Review of the Progress and Challenges of Developing a Vaccine for COVID-19.* Frontiers in Immunology, 2020. **11**(2413).
10. Guo, K., et al., *Interferon Resistance of Emerging SARS-CoV-2 Variants.* bioRxiv, 2021: p. 2021.03.20.436257.
11. Muik, A., et al., *Neutralization of SARS-CoV-2 lineage B.1.1.7 pseudovirus by BNT162b2 vaccine-elicited human sera.* bioRxiv, 2021: p. 2021.01.18.426984.
12. Wang, P., et al., *Increased Resistance of SARS-CoV-2 Variants B.1.351 and B.1.1.7 to Antibody Neutralization.* bioRxiv, 2021: p. 2021.01.25.428137.
13. Chang, X., et al., *BNT162b2 mRNA COVID-19 vaccine induces antibodies of broader cross-reactivity than natural infection but recognition of mutant viruses is up to 10-fold reduced.* bioRxiv, 2021: p. 2021.03.13.435222.
14. Smatti, M.K., et al., *Measuring influenza hemagglutinin (HA) stem-specific antibody-dependent cellular cytotoxicity (ADCC) in human sera using novel stabilized stem nanoparticle probes.* Vaccine, 2020. **38**(4): p. 815-821.
15. Liu, Q., et al., *Antibody-dependent-cellular-cytotoxicity-inducing antibodies significantly affect the post-exposure treatment of Ebola virus infection.* Sci Rep, 2017. **7**: p. 45552.
16. Pinto, D., et al., *Structural and functional analysis of a potent sarbecovirus neutralizing antibody.* bioRxiv : the preprint server for biology, 2020: p. 2020.04.07.023903.
17. Jegaskanda, S., *The Potential Role of Fc-Receptor Functions in the Development of a Universal Influenza Vaccine.* Vaccines, 2018. **6**(2): p. 27.
18. Vanderven, H.A., et al., *Antibody-dependent cellular cytotoxicity and influenza virus.* Curr Opin Virol, 2017. **22**: p. 89-96.
19. Wang, S.C., et al., *Development of a universal influenza vaccine using hemagglutinin stem protein produced from Pichia pastoris.* Virology, 2019.

526: p. 125-137.
20. Forthal, D.N. and A. Finzi, *Antibody-dependent cellular cytotoxicity in HIV infection.* AIDS (London, England), 2018. **32**(17): p. 2439-2451.
21. Kohl, S., et al., *Analysis of the role of antibody-dependent cellular cytotoxic antibody activity in murine neonatal herpes simplex virus infection with antibodies to synthetic peptides of glycoprotein D and monoclonal antibodies to glycoprotein B.* The Journal of clinical investigation, 1990. **86**(1): p. 273-278.
22. Phan, T., *Novel coronavirus: From discovery to clinical diagnostics.* Infection, Genetics and Evolution, 2020. **79**: p. 104211.
23. van Boheemen, S., et al., *Genomic characterization of a newly discovered coronavirus associated with acute respiratory distress syndrome in humans.* MBio, 2012. **3**(6).
24. Yan, Y., et al., *The First 75 Days of Novel Coronavirus (SARS-CoV-2) Outbreak: Recent Advances, Prevention, and Treatment.* International Journal of Environmental Research and Public Health, 2020. **17**(7).
25. Lim, Y.X., et al., *Human Coronaviruses: A Review of Virus-Host Interactions.* Diseases, 2016. **4**(3).
26. Fung, T.S. and D.X. Liu, *Human coronavirus: host-pathogen interaction.* Annual review of microbiology, 2019. **73**: p. 529-557.
27. Drosten, C., et al., *Identification of a novel coronavirus in patients with severe acute respiratory syndrome.* N Engl J Med, 2003. **348**(20): p. 1967-76.
28. Zaki, A.M., et al., *Isolation of a novel coronavirus from a man with pneumonia in Saudi Arabia.* N Engl J Med, 2012. **367**(19): p. 1814-20.
29. Chan, J.W., et al., *Short term outcome and risk factors for adverse clinical outcomes in adults with severe acute respiratory syndrome (SARS).* Thorax, 2003. **58**(8): p. 686-9.
30. WHO, *WHO MERS-CoV Global Summary and risk assessment*. 5 December 2016.
31. Cui, J., F. Li, and Z.-L. Shi, *Origin and evolution of pathogenic coronaviruses.* Nature reviews. Microbiology, 2019. **17**(3): p. 181-192.
32. Zaki, A.M., et al., *Isolation of a novel coronavirus from a man with pneumonia in Saudi Arabia.* New England Journal of Medicine, 2012. **367**(19): p. 1814-1820.
33. Li, W., et al., *Angiotensin-converting enzyme 2 is a functional receptor for the SARS coronavirus.* Nature, 2003. **426**(6965): p. 450-454.
34. Lu, G., et al., *Molecular basis of binding between novel human coronavirus MERS-CoV and its receptor CD26.* Nature, 2013. **500**(7461): p. 227-231.
35. Edridge, A.W.D., et al., *Seasonal coronavirus protective immunity is short-lasting.* Nature Medicine, 2020. **26**(11): p. 1691-1693.
36. De Wit, E., et al., *SARS and MERS: recent insights into emerging coronaviruses.* Nature Reviews Microbiology, 2016. **14**(8): p. 523-534.
37. Liu, D.X., J.Q. Liang, and T.S. Fung, *Human Coronavirus-229E, -OC43, -NL63, and -HKU1 (Coronaviridae).* Encyclopedia of Virology, 2021: p. 428-440.
38. Callow, K., et al., *The time course of the immune response to experimental coronavirus infection of man.* Epidemiology & Infection, 1990. **105**(2): p. 435-446.
39. Woudenberg, T., et al., *Humoral immunity to SARS-CoV-2 and seasonal coronaviruses in children and adults in north-eastern France.* EBioMedicine, 2021. **70**.

40. Corman, V.M., et al., *Viral shedding and antibody response in 37 patients with Middle East respiratory syndrome coronavirus infection.* Clinical Infectious Diseases, 2016. **62**(4): p. 477-483.
41. Buchholz, U., et al., *Contact investigation of a case of human novel coronavirus infection treated in a German hospital, October-November 2012.* Eurosurveillance, 2013. **18**(8): p. 20406.
42. Liu, W.J., et al., *T-cell immunity of SARS-CoV: Implications for vaccine development against MERS-CoV.* Antiviral research, 2017. **137**: p. 82-92.
43. Tang, F., et al., *Lack of peripheral memory B cell responses in recovered patients with severe acute respiratory syndrome: a six-year follow-up study.* The Journal of Immunology, 2011. **186**(12): p. 7264-7268.
44. Li, C.K.-f., et al., *T cell responses to whole SARS coronavirus in humans.* The Journal of Immunology, 2008. **181**(8): p. 5490-5500.
45. Lu, R., et al., *Genomic characterisation and epidemiology of 2019 novel coronavirus: implications for virus origins and receptor binding.* The Lancet, 2020. **395**(10224): p. 565-574.
46. Post, N., et al., *Antibody response to SARS-CoV-2 infection in humans: A systematic review.* PLOS ONE, 2021. **15**(12): p. e0244126.
47. Organization, W.H. *WHO Coronavirus Disease (COVID-19) Dashboard*. 2020 [cited 2020 1 July]; Available from: https://covid19.who.int/.
48. Mariano, G., et al., *Structural Characterization of SARS-CoV-2: Where We Are, and Where We Need to Be.* Frontiers in Molecular Biosciences, 2020. **7**(344).
49. Huang, Y., et al., *Structural and functional properties of SARS-CoV-2 spike protein: potential antivirus drug development for COVID-19.* Acta Pharmacologica Sinica, 2020. **41**(9): p. 1141-1149.
50. Zhu, N., et al., *A novel coronavirus from patients with pneumonia in China, 2019.* New England journal of medicine, 2020.
51. Cavanagh, D., *Coronaviridae: a review of coronaviruses and toroviruses.* Coronaviruses with Special Emphasis on First Insights Concerning SARS, 2005: p. 1-54.
52. Subbarao, K. and S. Mahanty, *Respiratory Virus Infections: Understanding COVID-19.* Immunity, 2020. **52**(6): p. 905-909.
53. Vardhana, S.A. and J.D. Wolchok, *The many faces of the anti-COVID immune response.* J Exp Med, 2020. **217**(6).
54. Mueller, S.N. and B.T. Rouse, *Immune responses to viruses.* Clinical Immunology, 2008: p. 421-431.
55. Zhu, J., H. Yamane, and W.E. Paul, *Differentiation of effector CD4 T cell populations (*).* Annu Rev Immunol, 2010. **28**: p. 445-89.
56. Lukacs, N.W. and C.A. Malinczak, *Harnessing Cellular Immunity for Vaccination against Respiratory Viruses.* Vaccines (Basel), 2020. **8**(4).
57. Dörner, T. and A. Radbruch, *Antibodies and B Cell Memory in Viral Immunity.* 2007.
58. Chen, X., et al., *The development and kinetics of functional antibody-dependent cell-mediated cytotoxicity (ADCC) to SARS-CoV-2 spike protein.* Virology, 2021. **559**: p. 1-9.
59. Yu, Y., et al., *Antibody-dependent cellular cytotoxicity response to SARS-CoV-2 in COVID-19 patients.* Signal Transduction and Targeted Therapy, 2021. **6**(1): p. 346.
60. Hessell, A.J., et al., *Fc receptor but not complement binding is important in antibody protection against HIV.* Nature, 2007. **449**(7158): p. 101-104.

61. Tso, F.Y., et al., *Presence of antibody-dependent cellular cytotoxicity (ADCC) against SARS-CoV-2 in COVID-19 plasma.* PLoS One, 2021. **16**(3): p. e0247640.
62. Grifoni, A., et al., *Targets of T cell responses to SARS-CoV-2 coronavirus in humans with COVID-19 disease and unexposed individuals.* Cell, 2020. **181**(7): p. 1489-1501. e15.
63. Wec, A.Z., et al., *Broad neutralization of SARS-related viruses by human monoclonal antibodies.* Science, 2020. **369**(6504): p. 731-736.
64. Pan, Y., et al., *SARS-CoV-2-specific immune response in COVID-19 convalescent individuals.* Signal Transduction and Targeted Therapy, 2021. **6**(1): p. 256.
65. Jiang, S., C. Hillyer, and L. Du, *Neutralizing antibodies against SARS-CoV-2 and other human coronaviruses.* Trends in immunology, 2020. **41**(5): p. 355-359.
66. Ibarrondo, F.J., et al., *Rapid decay of anti–SARS-CoV-2 antibodies in persons with mild Covid-19.* New England Journal of Medicine, 2020. **383**(11): p. 1085-1087.
67. Post, N., et al., *Antibody response to SARS-CoV-2 infection in humans: A systematic review.* PLoS One, 2020. **15**(12): p. e0244126.
68. Ma, H., et al., *Serum IgA, IgM, and IgG responses in COVID-19.* Cell Mol Immunol, 2020. **17**(7): p. 773-775.
69. Jääskeläinen, A.J., et al., *Evaluation of commercial and automated SARS-CoV-2 IgG and IgA ELISAs using coronavirus disease (COVID-19) patient samples.* Euro Surveill, 2020. **25**(18).
70. Qu, J., et al., *Profile of Immunoglobulin G and IgM Antibodies Against Severe Acute Respiratory Syndrome Coronavirus 2 (SARS-CoV-2).* Clin Infect Dis, 2020. **71**(16): p. 2255-2258.
71. Poland, G.A., et al., *SARS-CoV-2 Vaccine Development: Current Status.* Mayo Clinic proceedings, 2020. **95**(10): p. 2172-2188.
72. Excler, J.-L., et al., *Vaccine development for emerging infectious diseases.* Nature Medicine, 2021. **27**(4): p. 591-600.
73. Al-Jighefee, H.T., et al., *COVID-19 Vaccine Platforms: Challenges and Safety Contemplations.* Vaccines (Basel), 2021. **9**(10).
74. WHO, *Draft Landscape of COVID-19 Candidate Vaccines*. 2020, WHO: https://www.who.int/publications/m/item/draft-landscape-of-covid-19-candidate-vaccines.
75. Wisnewski, A.V., J. Campillo Luna, and C.A. Redlich, *Human IgG and IgA responses to COVID-19 mRNA vaccines.* PLoS One, 2021. **16**(6): p. e0249499.
76. Wang, Z., et al., *mRNA vaccine-elicited antibodies to SARS-CoV-2 and circulating variants.* Nature, 2021. **592**(7855): p. 616-622.
77. Barouch, D.H., et al., *Durable Humoral and Cellular Immune Responses 8 Months after Ad26.COV2.S Vaccination.* New England Journal of Medicine, 2021. **385**(10): p. 951-953.
78. Goel, R.R., et al., *Distinct antibody and memory B cell responses in SARS-CoV-2 naïve and recovered individuals following mRNA vaccination.* Sci Immunol, 2021. **6**(58).
79. Jackson, L.A., et al., *An mRNA Vaccine against SARS-CoV-2 — Preliminary Report.* New England Journal of Medicine, 2020. **383**(20): p. 1920-1931.
80. Walsh, E.E., et al., *Safety and Immunogenicity of Two RNA-Based Covid-19 Vaccine Candidates.* New England Journal of Medicine, 2020. **383**(25): p.

2439-2450.
81. Israel, A., et al., *Large-scale study of antibody titer decay following BNT162b2 mRNA vaccine or SARS-CoV-2 infection.* medRxiv, 2021.
82. Gilbert, P.B., et al., *Immune Correlates Analysis of the mRNA-1273 COVID-19 Vaccine Efficacy Trial.* medRxiv, 2021.
83. Frenck, R.W., et al., *Safety, Immunogenicity, and Efficacy of the BNT162b2 Covid-19 Vaccine in Adolescents.* New England Journal of Medicine, 2021. **385**(3): p. 239-250.
84. Chen, X., et al., *Comprehensive mapping of neutralizing antibodies against SARS-CoV-2 variants induced by natural infection or vaccination.* medRxiv, 2021.
85. Noori, M., et al., *Potency of BNT162b2 and mRNA-1273 vaccine-induced neutralizing antibodies against severe acute respiratory syndrome-CoV-2 variants of concern: A systematic review of in vitro studies.* Rev Med Virol, 2022. **32**(2): p. e2277.
86. Arora, P., et al., *B.1.617.2 enters and fuses lung cells with increased efficiency and evades antibodies induced by infection and vaccination.* Cell Rep, 2021. **37**(2): p. 109825.
87. Davis, C., et al., *Reduced neutralisation of the Delta (B.1.617.2) SARS-CoV-2 variant of concern following vaccination.* PLoS Pathog, 2021. **17**(12): p. e1010022.
88. Nasrallah, G.K., et al., *Seroprevalence of hepatitis E virus among blood donors in Qatar (2013-2016).* Transfusion, 2017. **57**(7): p. 1801-1807.
89. Smatti, M.K., et al., *Prevalence and molecular profiling of Epstein Barr virus (EBV) among healthy blood donors from different nationalities in Qatar.* PLoS One, 2017. **12**(12): p. e0189033.
90. Humphrey, J.M., et al., *Dengue and chikungunya seroprevalence among Qatari nationals and immigrants residing in Qatar.* PLoS ONE, 2019. **14**: p. e0211574.
91. Al-Qahtani, A.A., et al. *Prevalence of anelloviruses (TTV, TTMDV, and TTMV) in healthy blood donors and in patients infected with HBV or HCV in Qatar*. Virology journal, 2016. **13**, 208 DOI: 10.1186/s12985-016-0664-6.
92. Dargham, S.R., et al., *Herpes Simplex Virus Type 2 Seroprevalence Among Different National Populations of Middle East and North African Men.* Sexually transmitted diseases, 2018. **45**(7): p. 482-487.
93. Nasrallah, G.K., et al., *Estimating seroprevalence of herpes simplex virus type 1 among different Middle East and North African male populations residing in Qatar.* J Med Virol, 2018. **90**(1): p. 184-190.
94. Al Kahlout, R.A., et al., *Comparative Serological Study for the Prevalence of Anti-MERS Coronavirus Antibodies in High- and Low-Risk Groups in Qatar.* J Immunol Res, 2019. **2019**: p. 1386740.
95. Al-Thani, M.H., et al., *Seroprevalence of SARS-CoV-2 infection in the craft and manual worker population of Qatar.* medRxiv, 2020: p. 2020.11.24.20237719.
96. Syed, M.A., et al., *Epidemiology of SARS-CoV2 in Qatar's primary care population aged 10 years and above.* BMC Infectious Diseases, 2021. **21**(1): p. 645.
97. BIOMÉRIEUX, *VIDAS® SARS-COV-2*. 2020.
98. Wolff, F., et al., *Monitoring antibody response following SARS-CoV-2 infection: diagnostic efficiency of 4 automated immunoassays.* Diagnostic Microbiology and Infectious Disease, 2020. **98**(3): p. 115140.
99. Mindray. *SARS-CoV-2 IgG(CLIA)*. 2020; Available from:

https://www.mindray.com/en/product/CL-900i.html.
100. Nuccetelli, M., et al., *SARS-CoV-2 infection serology: a useful tool to overcome lockdown?* Cell Death Discovery, 2020. **6**(1): p. 38.
101. DiaSorin, *LIAISON® SARS-CoV-2 S1/S2 IgG.*
102. Bryan, A., et al., *Performance Characteristics of the Abbott Architect SARS-CoV-2 IgG Assay and Seroprevalence in Boise, Idaho.* Journal of clinical microbiology, 2020. **58**(8): p. e00941-20.
103. Chew, K.L., et al., *Clinical evaluation of serological IgG antibody response on the Abbott Architect for established SARS-CoV-2 infection.* Clinical Microbiology and Infection.
104. Meschi, S., et al., *Performance evaluation of Abbott ARCHITECT SARS-CoV-2 IgG immunoassay in comparison with indirect immunofluorescence and virus microneutralization test.* J Clin Virol, 2020. **129**: p. 104539.
105. Use, V.I.P.A.-S.-C.-T.R.P.-I.f. *VITROS Immunodiagnostic Products Anti-SARS-CoV-2 Total Reagent Pack - Instructions for Use*. 13 March 2021]; Available from: https://www.fda.gov/media/136967/download.
106. Perera, R.A.P.M., et al., *Evaluation of a SARS-CoV-2 surrogate virus neutralization test for detection of antibody in human, canine, cat and hamster sera.* Journal of Clinical Microbiology, 2020: p. JCM.02504-20.
107. Tan, C.W., et al., *A SARS-CoV-2 surrogate virus neutralization test based on antibody-mediated blockage of ACE2–spike protein–protein interaction.* Nature Biotechnology, 2020. **38**(9): p. 1073-1078.
108. Younes, S., et al., *Diagnostic Efficiency of Three Fully Automated Serology Assays and Their Correlation with a Novel Surrogate Virus Neutralization Test in Symptomatic and Asymptomatic SARS-COV-2 Individuals.* Microorganisms, 2021. **9**(2): p. 245.
109. Condor Capcha, J.M., et al., *Generation of SARS-CoV-2 Spike Pseudotyped Virus for Viral Entry and Neutralization Assays: A 1-Week Protocol.* Frontiers in Cardiovascular Medicine, 2021. **7**.
110. Nie, J., et al., *Quantification of SARS-CoV-2 neutralizing antibody by a pseudotyped virus-based assay.* Nature Protocols, 2020. **15**(11): p. 3699-3715.
111. Dufloo, J., et al., *Asymptomatic and symptomatic SARS-CoV-2 infections elicit polyfunctional antibodies.* Cell Rep Med, 2021. **2**(5): p. 100275.
112. *The Measurement of Interrater Agreement*, in *Statistical Methods for Rates and Proportions*. p. 598-626.
113. Mukaka, M.M., *Statistics corner: A guide to appropriate use of correlation coefficient in medical research.* Malawi medical journal : the journal of Medical Association of Malawi, 2012. **24**(3): p. 69-71.
114. Mandrekar, J.N., *Receiver Operating Characteristic Curve in Diagnostic Test Assessment.* Journal of Thoracic Oncology, 2010. **5**(9): p. 1315-1316.
115. Schisterman, E.F., et al., *Youden Index and the optimal threshold for markers with mass at zero.* Statistics in medicine, 2008. **27**(2): p. 297-315.
116. Unal, I., *Defining an Optimal Cut-Point Value in ROC Analysis: An Alternative Approach.* Computational and Mathematical Methods in Medicine, 2017. **2017**: p. 3762651.
117. Al-Jighefee, H.T., et al., *Evaluation of Antibody Response in Symptomatic and Asymptomatic COVID-19 Patients and Diagnostic Assessment of New IgM/IgG ELISA Kits.* Pathogens, 2021. **10**(2): p. 161.
118. Younes, S., et al., *Diagnostic Efficiency of Three Fully Automated Serology Assays and Their Correlation with a Novel Surrogate Virus Neutralization Test*

in Symptomatic and Asymptomatic SARS-COV-2 Individuals. Microorganisms, 2021. **9**(2).
119. Ismail, A., et al., *Can commercial automated immunoassays be utilized to predict neutralizing antibodies after SARS-CoV-2 infection? A comparative study between three different assays.* 2021.
120. Whitman, J.D., et al., *Evaluation of SARS-CoV-2 serology assays reveals a range of test performance.* Nature Biotechnology, 2020. **38**(10): p. 1174-1183.
121. CDC, U., *Interim Guidelines for COVID-19 Antibody Testing*. Jan. 24, 2022: https://www.cdc.gov/coronavirus/2019-ncov/lab/resources/antibody-tests-guidelines.html.
122. Serre-Miranda, C., et al., *Performance assessment of 11 commercial serological tests for SARS-CoV-2 on hospitalized COVID-19 patients.* medRxiv, 2020: p. 2020.08.06.20168856.
123. Kweon, O.J., et al., *Antibody kinetics and serologic profiles of SARS-CoV-2 infection using two serologic assays.* PLOS ONE, 2020. **15**(10): p. e0240395.
124. Zhao, J., et al., *Antibody responses to SARS-CoV-2 in patients of novel coronavirus disease 2019.* Clin Infect Dis, 2020.
125. Long, Q.-X., et al., *Antibody responses to SARS-CoV-2 in patients with COVID-19.* Nature Medicine, 2020. **26**(6): p. 845-848.
126. Zeng, F., et al., *Quantitative comparison of the efficiency of antibodies against S1 and S2 subunit of SARS coronavirus spike protein in virus neutralization and blocking of receptor binding: implications for the functional roles of S2 subunit.* FEBS Lett, 2006. **580**(24): p. 5612-20.
127. Premkumar, L., et al., *The receptor binding domain of the viral spike protein is an immunodominant and highly specific target of antibodies in SARS-CoV-2 patients.* Sci Immunol, 2020. **5**(48).
128. Robbiani, D.F., et al., *Convergent antibody responses to SARS-CoV-2 in convalescent individuals.* Nature, 2020. **584**(7821): p. 437-442.
129. Gunn, B.M., et al., *A role for Fc function in therapeutic monoclonal antibody-mediated protection against Ebola virus.* Cell host & microbe, 2018. **24**(2): p. 221-233. e5.
130. Vanderven, H.A. and S.J. Kent, *The protective potential of Fc-mediated antibody functions against influenza virus and other viral pathogens.* Immunology and Cell Biology, 2020. **98**(4): p. 253-263.
131. Terajima, M., et al., *High antibody-dependent cellular cytotoxicity antibody titers to H5N1 and H7N9 avian influenza A viruses in healthy US adults and older children.* The Journal of infectious diseases, 2015. **212**(7): p. 1052-1060.
132. Poppe, L.K., C. Wood, and J.T. West, *The presence of antibody-dependent cell cytotoxicity–mediating antibodies in Kaposi sarcoma–associated herpesvirus–seropositive individuals does not correlate with disease pathogenesis or progression.* The Journal of Immunology, 2020. **205**(10): p. 2742-2749.
133. Grudzien, M. and A. Rapak, *Effect of natural compounds on NK cell activation.* Journal of Immunology Research, 2018. **2018**.
134. Li, S.S., et al., *FCGR2C polymorphisms associate with HIV-1 vaccine protection in RV144 trial.* The Journal of clinical investigation, 2014. **124**(9): p. 3879-3890.
135. Laoprasopwattana, K., et al., *Antibody-dependent cellular cytotoxity mediated by plasma obtained before secondary dengue virus infections: Potential involvement in early control of viral replication.* The Journal of infectious diseases, 2007. **195**(8): p. 1108-1116.

136. Huber, V.C., et al., *Fc receptor-mediated phagocytosis makes a significant contribution to clearance of influenza virus infections.* The Journal of Immunology, 2001. **166**(12): p. 7381-7388.
137. Khurana, S., et al., *Vaccine-induced anti-HA2 antibodies promote virus fusion and enhance influenza virus respiratory disease.* Science translational medicine, 2013. **5**(200): p. 200ra114-200ra114.
138. Co, M.D.T., et al., *Relationship of preexisting influenza hemagglutination inhibition, complement-dependent lytic, and antibody-dependent cellular cytotoxicity antibodies to the development of clinical illness in a prospective study of A (H1N1) pdm09 Influenza in children.* Viral immunology, 2014. **27**(8): p. 375-382.
139. Lu, L.L., et al., *Beyond binding: antibody effector functions in infectious diseases.* Nature Reviews Immunology, 2018. **18**(1): p. 46-61.
140. Yao, L., et al., *Persistence of Antibody and Cellular Immune Responses in Coronavirus Disease 2019 Patients Over Nine Months After Infection.* J Infect Dis, 2021. **224**(4): p. 586-594.
141. Wu, K., et al., *mRNA-1273 vaccine induces neutralizing antibodies against spike mutants from global SARS-CoV-2 variants.* bioRxiv, 2021: p. 2021.01.25.427948.
142. Chmielewska, A.M., et al., *Immune response against SARS-CoV-2 variants: the role of neutralization assays.* npj Vaccines, 2021. **6**(1): p. 142.
143. Tauzin, A., et al., *A single dose of the SARS-CoV-2 vaccine BNT162b2 elicits Fc-mediated antibody effector functions and T cell responses.* Cell host & microbe, 2021. **29**(7): p. 1137-1150. e6.
144. Pinto, D., et al., *Cross-neutralization of SARS-CoV-2 by a human monoclonal SARS-CoV antibody.* Nature, 2020. **583**(7815): p. 290-295.
145. Pinto, D., et al., *Broad betacoronavirus neutralization by a stem helix-specific human antibody.* Science, 2021. **373**(6559): p. 1109-1116.
146. Tharakaraman, K., et al., *A broadly neutralizing human monoclonal antibody is effective against H7N9.* Proc Natl Acad Sci U S A, 2015. **112**(35): p. 10890-5.

APPENDIXES

Appendix 1:

Table S1. Characteristics of the evaluated CE-marked ELISA kits, including the recombinant antigen used, immunoglobulin (Ig) classes, and the reported sensitivity and specificity by the company.

Assay	Manufacturer	Detected Antibody	Principle of Detection	Antigen/Antibody Coating the Plate	Reported Sensitivity	Reported Specificity
EDI™ Novel Coronavirus COVID-19 ELISA Kit	Epitope Diagnostics, Inc.	IgM	Capture ELISA	Anti-human IgM specific capture antibody	45% (vs. RT-PCR [1])	100% (vs. PCR)
		IgG	Indirect ELISA	Recombinant full length nucleocapsid protein	100% (vs. RT-PCR)	100% (vs. PCR)
NovaLisa® SARS-CoV-2 ELISA	NovaLisa Immundiagnostica GmbH	IgM	Indirect ELISA	Recombinant nucleocapsid antigen	0–30% (<11 days) 40% (≥12 days) (vs. RT-PCR)	100%
		IgG	Indirect ELISA	Recombinant nucleocapsid antigen	8–40% (<11 days) 100% (≥12 days) (vs. RT-PCR)	99.3%
AnshLabs SARS-CoV-2 ELISA	AnshLabs	IgM	Capture ELISA	Anti-human IgM specific capture antibody	100% (vs. CLIA [2]) 40% (vs. RT-PCR)	98.5% (vs. CLIA) 100% (vs. PCR)

		IgG	Indirect ELISA	Recombinant nucleocapsid and spike antigens	95% (vs. CLIA) 83.6% (vs. RT-PCR)	98.3% (vs. CLIA) 91.3% (vs. PCR)
DiaPro COVID-19 ELISA	Diagnostic Bioprobes	IgG	Indirect ELISA	Recombinant nucleocapsid and spike antigens	≥98% (vs. RT-PCR)	≥98%
Lionex COVID-19 ELISA	Lionex Diagnostics and Therapeutics	IgM	Indirect ELISA	Recombinant S1 antigen	62.5% (vs. RT-PCR)	97.9%
		IgG	Indirect ELISA	Recombinant S1 antigen	>84% (vs. RT-PCR)	99.35%

[1] RT–PCR: real-time polymerase chain reaction. [2] CLIA: chemiluminescent immunoassay.

Appendix 2:

Table S2. The diagnostic assessment of IgG and IgM ELISA kits with real-time polymerase chain reaction (RT-PCR) at the three-time intervals (≤14, 14-30, >30 days) and in symptomatic/asymptomatic coronavirus disease 2019 (COVID-19) patients (n=291).

Diagnostic assessment	**IgG ELISA**					**IgM ELISA**			
	EDI	**NovaLisa**	**AnshLabs**	**DiaPro**	**Lionex**	**EDI**	**NovaLisa**	**AnshLabs**	**Lionex**
Sensitivity **≤14** DPSO/DPD[1]	**49.6%** (59/119, 40.6-58.6)	**61.0%** (61/100, 51.4-70.6)	**78.2%** (93/119, 70.7-85.6)	**48.7%** (58/119, 39.8-57.7)	**58.6%** (58/99, 48.9-68.3)	**48.7%** (58/119, 39.8-57.7)	**46.2%** (55/119, 37.3-55.2)	**53.8%** (64/119, 44.8-62.8)	**66.4%** (79/119, 57.9-74.9)
Sensitivity **14-30** DPSO/DPD[1]	**61.8%** (34/55, 49.0-74.7)	**81.5%** (44/54, 71.1-91.8)	**83.6%** (46/55, 73.9-93.4)	**60.0%** (33/55, 47.1-72.9)	**81.5%** (44/54, 71.1-91.8)	**34.5%** (20/55, 22.0-47.1)	**29.1%** (16/55, 17.1-41.1)	**38.2%** (21/55, 25.3-51.0)	**61.8%** (34/55, 49.0-74.7)
Sensitivity **>30** DPSO/DPD[1]	**76.1%** (89/117, 68.3-83.8)	**90.0%** (99/110, 84.4-95.6	**95.7%** (112/117, 92.1-99.4)	**53.5%** (38/71, 41.9-65.1)	**96.6%** (113/117, 93.3-99.9)	**10.3%** (12/117, 4.8-15.8)	**12.8%** (15/117, 6.8-18.9)	**6.8%** (8/117, 2.3-11.4)	**47.9%** (56/117, 38.8-56.9)
Sensitivity in **symptomatic** COVID-19 patients	**71.4%** (104/147, 64.1-78.7)	**84.1%** (111/132, 77.9-90.3)	**89.1%** (131/147, 84.1-94.2)	**67.3%** (99/147, 59.8-74.9)	**84.1%** (111/132, 77.9-90.3)	**52.4%** (77/147, 44.3-60.5)	**45.6%** (67/147, 37.5-53.6)	**57.1%** (84/147, 49.1-65.1)	**75.5%** (111/147, 68.6-82.5)

Sensitivity in **asymptomatic** COVID-19 patients	**56.0%** (65/116, 47.0-65.1)	**67.9%** (74/109, 59.1-76.7)	**86.2%** (100/116, 79.9-92.5)	**24.3%** (18/70, 14.2-34.3)	**71.6%** (83/116, 63.3-79.8)	**7.8%** (9/116, 2.9-12.6)	**13.8%** (16/116, 7.5-20.1)	**3.4%** (4/116, 0.13-6.8)	**39.7%** (46/116, 30.8-48.6)
Overall sensitivity	**62.5%** (182/291, 57.0-68.1)	**77.6%** (204/263, 72.5-82.6)	**86.3%** (251/291, 82.3-90.2)	**52.7%** (129/245, 46.4-58.9)	**80.0%** (216/270, 75.2-84.8)	**30.6%** (89/291, 25.3-35.9)	**29.6%** (86/291, 24.3-34.8)	**31.6%** (92/291, 26.3-37.0)	**58.4%** (170/291, 52.8-64.1)
Overall agreement with RT-PCR	**72.9%** (68.6-77.2)	**83.5%** (79.8-87.2)	**85.6%** (82.2-89.0)	**60.2%** (55.1-65.2)	**85.3%** (81.8-88.9)	**50.5%** (45.6-55.3)	**46.8%** (42.0-51.7)	**50.0%** (45.2-54.8)	**67.1%** (62.5-71.6)
Positive predictive value	**98.9%** (97.9-99.9)	**98.1%** (96.7-99.5)	**93.0%** (90.5-95.4)	**81.6%** (77.6-85.6)	**98.6%** (97.5-99.8)	**98.9%** (97.8-99.9)	**86.9%** (83.6-90.1)	**93.9%** (91.6-96.2)	**92.4%** (89.8-94.9)
Negative predictive value	**51.8%** (46.9-56.6)	**66.1%** (61.3-70.8)	**71.4%** (67.1-75.8)	**43.7%** (38.6-48.8)	**68.2%** (63.6-72.9%)	**36.9%** (32.2-41.5)	**34.1%** (29.5-38.7)	**36.2%** (31.6-40.9)	**46.5%** (41.6-51.3)

[1]DPSO: Days post symptoms onset, DPD: days post diagnosis.

Appenix 3: Similarity index report

thesis

ORIGINALITY REPORT

20%
SIMILARITY INDEX

PRIMARY SOURCES

1	qspace.qu.edu.qa Internet	83 words — < 1%
2	www.premilife.com Internet	80 words — < 1%
3	academic.oup.com Internet	76 words — < 1%
4	disco.uni-muenster.de Internet	72 words — < 1%
5	bmcpublichealth.biomedcentral.com Internet	67 words — < 1%
6	Guoqiang Liu, James F. Rusling. "COVID-19 Antibody Tests and Their Limitations", ACS Sensors, 2021 Crossref	66 words — < 1%
7	Mary-Anne Trabaud, Vinca Icard, Marie-Paule Milon, Antonin Bal, Bruno Lina, Vanessa Escuret. "Comparison of eight commercial, high-throughput, automated or ELISA assays detecting SARS-CoV-2 IgG or total antibody", Journal of Clinical Virology, 2020 Crossref	66 words — < 1%
8	poligene.com.br Internet	